An Abstract of the Thesis of

Peter John Jensen for the degree of Master of Science in Nuclear Engineering presented on December 8, 1983

Title: A RETRAN Model for a Hypothetical Steam Line Break Occurring at Low Power Operation of the Trojan Nuclear Plant

Abstract Approved: Redacted for Privacy

The goal of this study is the modeling of a postulated break of the steam line at the containment penetration of the Trojan Nuclear Plant which is owned and operated by Portland General Electric. To perform this modeling, the RETRAN computer code package was utilized. RETRAN is designed to provide a best-estimate thermal hydraulic analysis of complex fluid flow systems such as those associated with light water reactors, solving both steady state and time dependent problems. A one loop RETRAN model of the Trojan Nuclear Plant including both a primary system and one steam generator had been developed previously at Oregon State University and was used as a starting point.

The first step of this study was the refinement of the model into a two loop model. Since Trojan has four actual loops, one modeling loop represents three actual loops and the other modeling loop represents one actual loop. This allows the simulation of a transient introduced in one loop only, in contrast to the one loop model which requires introduction of the transient in all four loops simultaneously

The second step in this study was to establish a steady state solution at four percent power consistent with the 100 percent power solution. Since the steam generator outlet pressure increases as power decreases, steam line break flow rates will be higher at low power, yielding a more conservative result (higher

mass and energy release rates). Although hot standby (zero power) implies the highest outlet pressure, four percent power was used for modeling convenience: fewer alterations to the existing model were required with no loss of accuracy.

The final step of the study consisted of including the steam lines in the RETRAN model and the simulation of a steam line break at a weld at the penetration of the primary containment. This weld was of particular interest because its location makes inspection and maintenance difficult. The transient was modeled for the relatively short time span of two seconds since maximum flow and energy release rates occurring during this interval were of primary interest.

A RETRAN Model for a Hypothetical Steam Line Break Occurring at Low Power Operation of the Trojan Nuclear Plant

By

Peter John Jensen

A Thesis
submitted to

Oregon State University

in partial fulfillment of
the requirements for the
degree of
Master of Science

Completed December 8, 1983
Commencement June 1983 [ie: 1984]

APPROVED:

Redacted for Privacy

Professor of Nuclear Engineering in charge of major

Redacted for Privacy

Head of Department of Nuclear Engineering

Redacted for Privacy

Dean of Graduate School

Date thesis is presented December 8, 1983

Typed by Peter Jensen

TABLE OF CONTENTS

LIST OF FIGURES

Figure Page

List of Tables

A RETRAN Model for a Hypothetical Steam Line Break Occurring at Low Power Operation of the Trojan Nuclear Plant

1. Introduction

The main objectives of this study were

1) The refinement of a one loop RETRAN PWR model as listed in reference 1 by expanding the model to two loops.
2) The establishment of steady state initial conditions at four percent power, consistent with rated power conditions.
3) The addition of steam lines to the model for the purpose of simulating a steam line break at the penetration of the primary containment.

Numerical values of input parameters for this model are referenced to the Trojan Nuclear Plant owned and operated by Portland General Electric (PGE).

The one loop model was expanded into a two loop model such that one of these loops (triple loop) represents three actual loops, and the other loop (single loop) represents one actual loop. The two loop model allows the realistic simulation of a greater number of transients than a one loop model since the two loop model allows different effects between the single loop and triple loop where as the single loop model can only accommodate transients which affect all four loops in the same way.

Since the secondary steam outlet pressure increases with decreasing power level, a steam line break at low power will yield higher mass and energy release rates than a break at high power. The highest pressure prevails at hot standby operation; however, the transient in this study was run from steady state operation at four percent power for convenience: a subcritical reactor (as would be the case at hot standby) is not included among the initial

steady state conditions which can be specified to the RETRAN code. Therefore, representation of decay heat present at hot standby must be done by one of two methods: 1) by entering the core heat release as a fuction of time, 2) by setting the core power (in a critical state) to a level representative of the decay heat release at hot standby. Since the transient in this study lasts only two seconds, there is no difference between these two methods with respect to steam line break flow rates so long as the power specified for each method is the same. Because the RETRAN model being used already included a critical core model (point kinetics without feedback considerations), it was found more convenient to keep this model and simply prescribe a power level of four percent (which is equivalent to the decay heat release rate about one minute after a reactor scram), and set the steam generator pressure equal to the pressure at hot standby.

Several modeling variations, each with its own assumptions about the nature of the break have been employed. This was done to widen the scope of the study and to expose the sensitivity of the results to variations in the modeling assumptions.

Due to the nature of this particular transient immediately after the pipe rupture, most graphs are presented on a semi-log scale with respect to time as this type of plot reflects both the prompt and long range response. Graphing was done using linear interpolation of computed data points.

2. RETRAN Model Description

2.1 Primary System and Steam Generators

The two loop RETRAN model for Trojan was obtained by expanding the model that is listed in reference 1 into a a model with a single and a triple loop as shown in Fig. 1. The triple loop is modeled with volumes and other related system parameters (initial flow rates, flow areas, etc.) equal to three times those of the single loop. Table 1 lists relevant RETRAN input parameters for the two loop model relative to those of the one loop model. The model is formulated so that the pressurizer can be associated with either the single or the triple loop.

Since this study covers only the first two seconds of the transient, a detailed representation of the reactor core is unnecessary; it is modeled as in reference 1 with two flow volumes (including a bypass volume) and one fuel node without feedback considerations.

2.2 Steam Lines

The four Trojan steam lines consist of two pairs of nearly identical piping runs, one pair being 14 feet shorter than the other. One steam line from each pair is shown in Fig. 2. In keeping with the previously described model split, three steam lines were allocated to the triple steam generator and one was associated with the single steam generator; however, since Trojan

---

1) Additional minor changes and corrections are discussed in appendix I

does not have three steam lines of equal length, some modeling adjustments were made. One of the longer lines was made equivalent to the two shorter lines, and these three combined were attached to the triple steam generator. Shortening one steam line is not unreasonable since it involves a small adjustment (about 14 feet out of 170 feet total) in a location far removed from the break assumed to occur in the single steam line. In a two second transient this adjustment would have negligible effect on break conditions. Loss coefficients for flow restrictors and bends in the steam lines were found through calculations using reference 2 or by taking known values from similar structures when data was insufficient for calculation. When the position of a bend in Trojan piping did not correspond to a RETRAN junction location, the associated loss coefficient was simply assigned to the nearest RETRAN junction.

Nodalization of the steam lines was done by considering three criteria: 1) compatability with the model already in existence, 2) accuracy of results, 3) computer time required for each RETRAN run. Since computing time for a given case is roughly proportional to the number of volumes, there is considerable incentive to reduce the number of volumes to a minimum while maintaining acceptable accuracy. Compatability with the already existing model implies flow lengths of the steam line volumes to be roughly equivalent to those of the primary and secondary systems, since excessively fine nodalization would be wasted once the steam line break flow conditions become dominated by steam generator conditions; however, fine nodalization will give more accurate results in the early phase of the transient, which is important. When representing a continuous phenomenon (such as fluid flow) in a discrete manner (as in RETRAN), distorted frequency and reduced resolution of results occurs and becomes more pronounced as the discretization becomes more coarse. A block diagram of the steam lines as represented in

---

2) A similar situation is the use of only a few terms in a Fourier series solution to a partial differential equation.

the RETRAN model is shown in Fig. 3.

The venturis (steam flow restrictors) located in the steam lines near the steam generators are modeled as RETRAN junctions with loss coefficients of 0.35, and areas equal to the venturi throat areas; choked flow conditions occuring at these junctions are modeled by the isoenthalpic expansion model provided by RETRAN.

RETRAN offers two types of check valve models: Type 0 without a hysteresis loop in the flow-versus-pressure curve; and Type 1 with the hysteresis loop, which was chosen for this model. The characteristic curves for these two types are shown in Fig. 4. Both options involve flow dependent pressure losses of the form

$$P = (CVi)W|W|/\rho$$

where W is the mass flow rate through the valve, ρ is the fluid density, and the CVi's are three input parameters:

1) CV1 is used for positive flow with the valve open.
2) CV2 is used for negative flow with the valve open.
3) CV3 is used for negative flow with the valve almost closed (leakage).

Because the pressure drop across the valve is proportional to CVi as well as to $W|W|$, W will be halved if CVi is multiplied by four, for a given pressure drop and density, as was verified by test calculations.

For negative flow, the valve remains open if the pressure loss, which is proportional to CV2, is less than the back pressure, Pcv (a RETRAN input parameter), required to close the valve. When Pcv is reached, the valve closes and the pressure loss becomes proportional to CV3.

A Type 1 valve remains closed until the pressure loss across the closed valve (proportional to CV3) is less than Pcv, where the Type 0 valve reopens when the pressure drop calculated assuming the valve is actually open (proportional to CV2) is less than Pcv, which is exactly the reverse of the Type 0 valve closing process. With the Type 1 valve, reopening never occured in any of the cases studied here, and it is not expected that a Type 0 valve would have

opened if it had been used instead of the Type 1 valve.

For this study, Pcv was chosen as 0.1 psi, both CV1 and CV2 were 1.0, and CV3 was 1.0E+5 or 1.0E+6 (see appendix I).

Downstream from the checkvalve is an "infinite" volume which represents the remaining sections of the steamlines, turbine, and other system components. Algorithms in RETRAN assume an "infinite" volume to be at a constant state regardless of flow in or out of it. The infinite volume was specified to have an enthalpy approximately equal to the steam enthalpy at the checkvalve (at normal four percent power conditions). The volume pressure is then determined by the steady state initialization procedure as being slightly less than the upstream pressure (volume 251) such that the specified flow is achieved. In an actual transient, the check valve will close after flow reversal and a small leak flow will issue through the valve from the steam line downstream (from the initial flow direction). The actual conditions of the steam downstream from the checkvalve are approximated in this model by those of the constant infinite volume. When reverse flow and leakage occur, actual conditions behind the checkvalve will change; however, since the significant phase of the transient lasts only two seconds, and since the leak flow is only a few tens of pounds per second compared with several thousand pounds per second for the total break flow, any change in actual conditions past the checkvalve will not cause a significant deviation between actual and model results.

Input Parameter	Triple Loop Value	Single Loop Value
Volume & Junction Flow Areas	0.75	0.25
Volume Hydraulic Diameters	1.0	1.0
Volume & Junction Elevations	1.0	1.0
Volume Size	0.75	0.25
Volume Height	1.0	1.0
Volume Mixture Levels	1.0	1.0
Mass Flow Rates	0.75	0.25
Junction Inertias	1.33	4.0
Loss Coefficients	1.0	1.0
Rated Pump Flow Rate	0.75	0.25
Rated Pump Torque	0.75	0.25
Pump Inertia	0.75	0.25
Steam Generator Heat Transfer Area	0.75	0.25
Steam Generator U-tube Volume	0.75	0.25
Fraction of Power Removed	0.75	0.25

Table 1. RETRAN Input Parameters for the Two Loop Model Relative to the One Loop Model Values

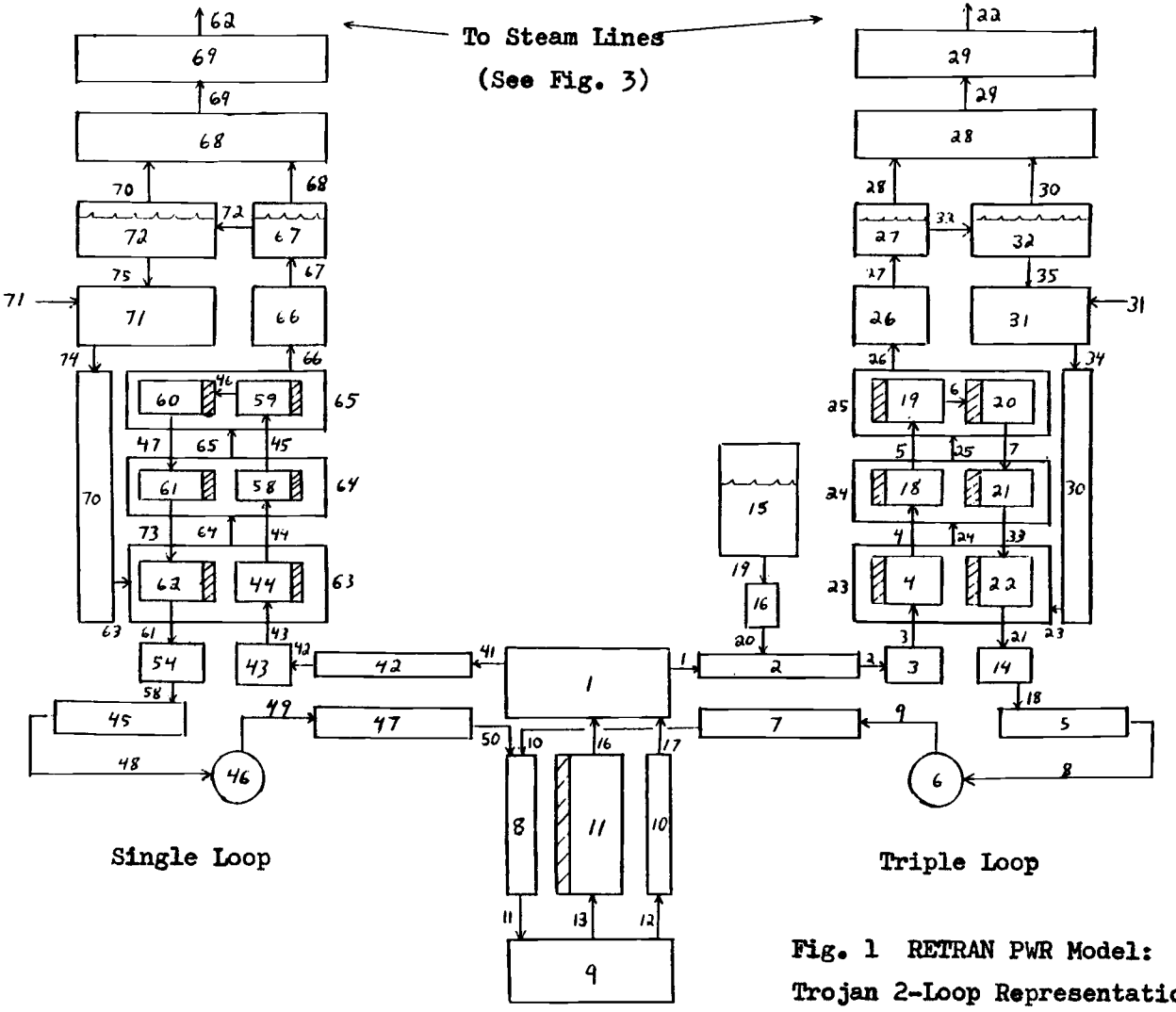

Fig. 1 RETRAN PWR Model:
Trojan 2-Loop Representation

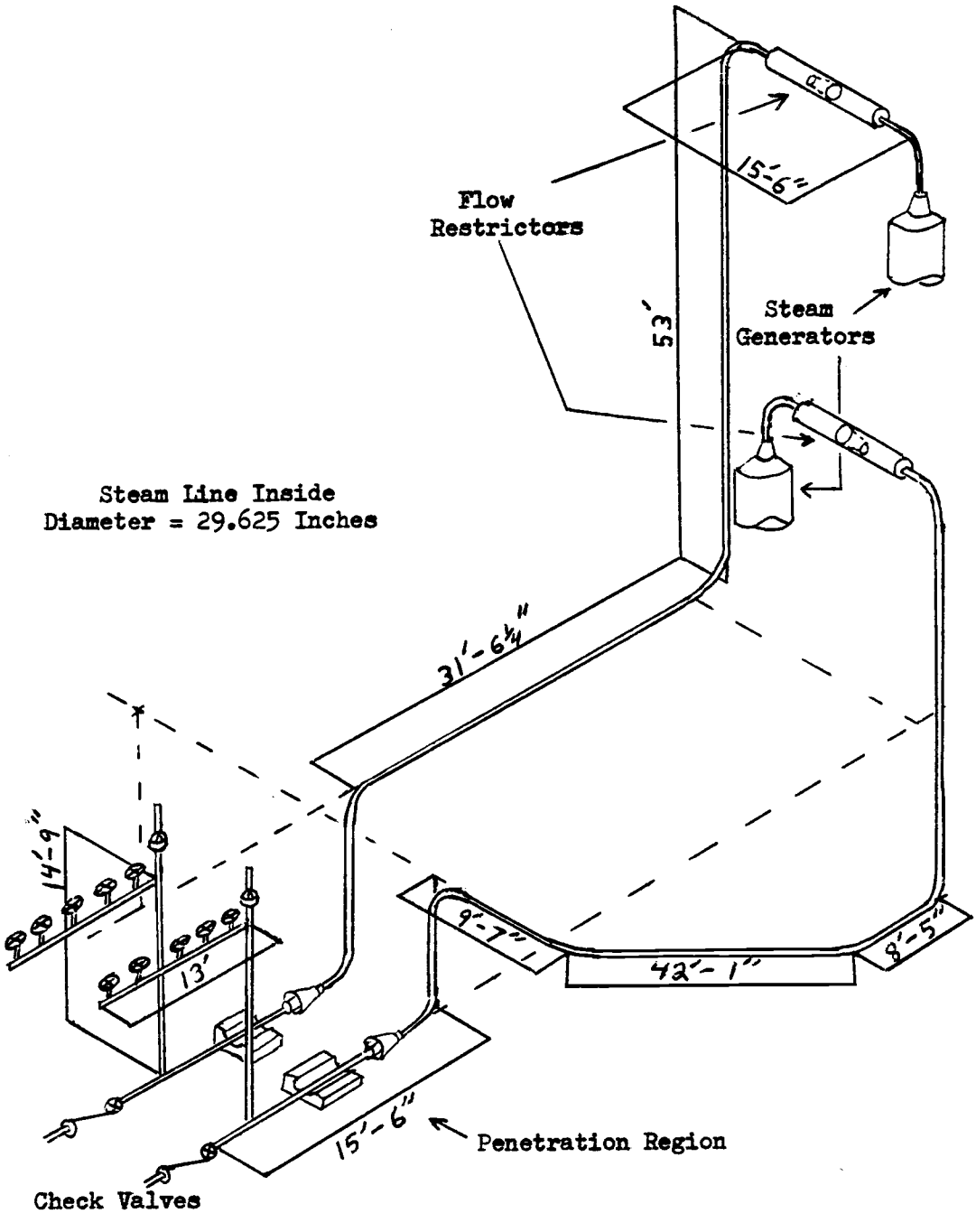

Fig. 2 Steam Lines (Portion Included in Model)

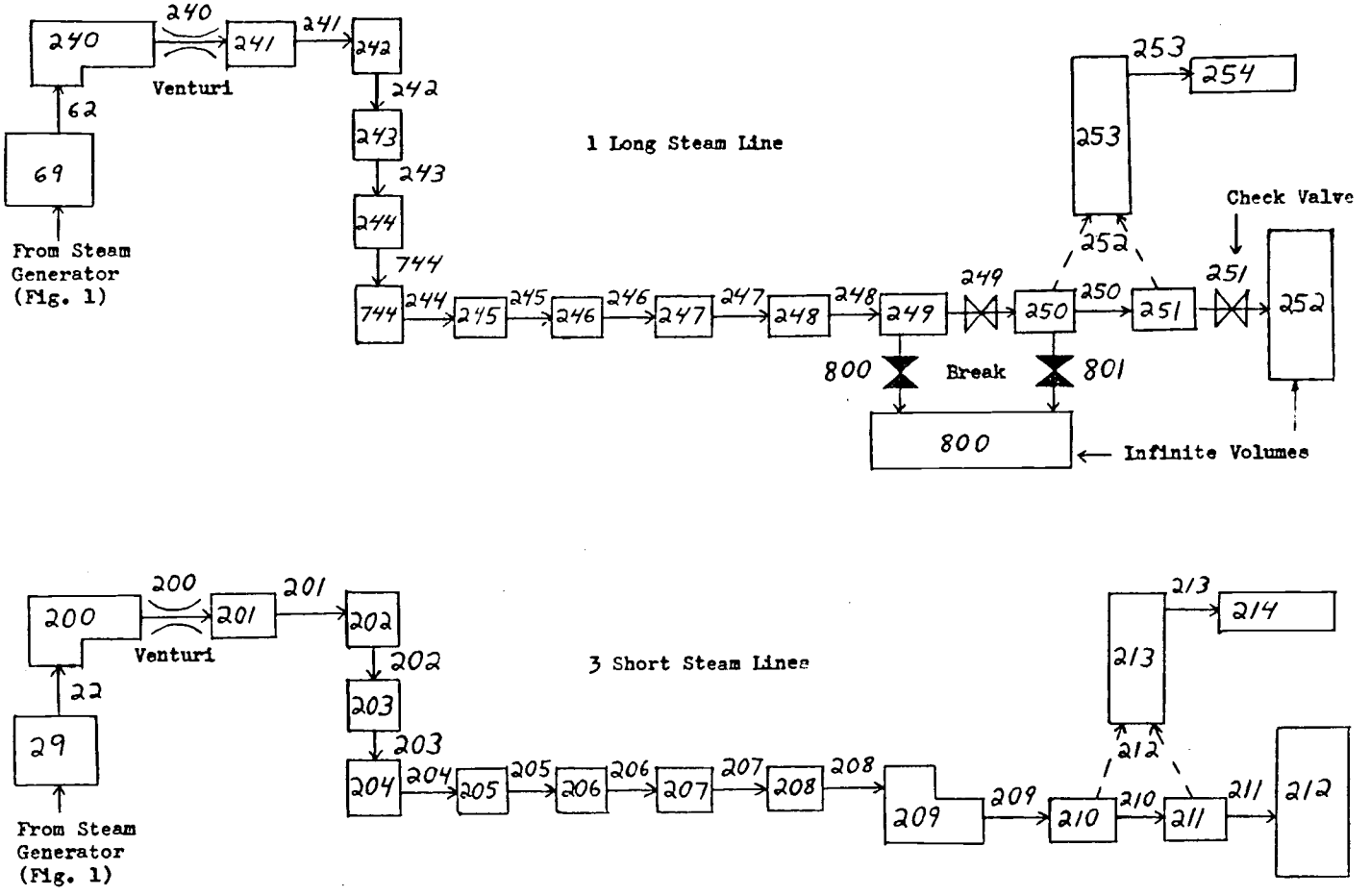

Fig. 3 Steam Lines and Break

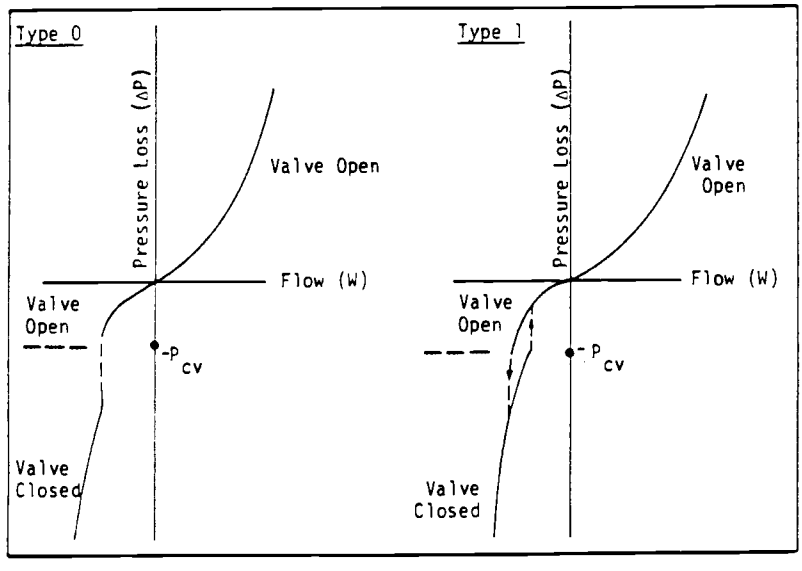

Fig. 4 Check Valve Characteristic Curves (Reference 3)

3. Initial Conditions

As previously mentioned, one of the objectives of this study was the establishment of a steady state solution at four percent power. For this purpose it was necessary to establish pressures, enthalpies, and flow rates on primary and secondary sides representative of the Trojan plant operating at four percent power.

As mentioned in reference 1, the loss coefficients at junctions 23 and 28 (and corresponding junctions 63 and 68) are left unspecified in the RETRAN input and are computed by the steady state self initialization feature of the code. Since loss coefficients are representative of the geometry of the flow path, they must be regarded as being invariant to operating conditions of a given system. Thus, a reasonable steady state solution at four percent power will require all unspecified loss coefficients to equal those calculated for a full power solution. The principal parameter varied to achieve the desired junction 23 and 63 loss coefficients is the recirculation ratio (ratio of mass flow rate entering the tube bundle region to the feed/steam mass flow rate), while the main parameter useful in adjusting the juntion 28 and 68 loss coefficients is the liquid level in volumes 27 and 67 respectively.

Another consideration in reaching a desired solution is the comparison of the calculated U-tube heat transfer area with the actual heat transfer area. In the RETRAN steady state initialization, both primary and secondary systems are completely specified, as are all heat transfer correlations. Since the power transferred through U-tubes is known, the system is overspecified. For example, with given conditions on the primary side, a certain amount of heat will be transferred through the U-tubes when the RETRAN heat transfer correlations are used; however, this amount of heat transfer may differ from the amount of heat released to the primary side by the core and reactor coolant pumps. To alleviate

this problem, RETRAN calculates and uses an adjusted (effective) heat transfer area such that the desired steady state power will be transmitted. One portion of arriving at a reasonable steady state solution is finding the value of relevant input parameters such that the calculated heat transfer areas agree closely with the actual heat transfer areas for all power levels. The principal parameter available for accomplishing this goal is the temperature level of the primary system coolant as determined by the inlet plenum (volume 9) enthalpy.

The final concern in establishing a steady state was the steam carry-under (the weight percent of entrained steam which is drawn out of the moisture separators and enters the downcomer - i.e. the weight percent of steam at junctions 35 and 75), which is assumed to be less than 0.5 percent of the total steam flow for all power levels, including those used in this study. The pricipal parameter useful in steam carry-under adjustment is the enthalpy of the secondary coolant in the steam generator mixing volumes (volumes 31 and 71).

Table 2 lists the input parameters adjusted to achieve a consistent steady state solution, and their corresponding dependent variables. Although there was some interplay between all of the input parameters and each of the dependent variables, each dependent variable was affected significantly by only one of the input parameters. Figures 5, 6, and 7 indicate the behavior of the dependent variables when compared with their principal independent input parameters (using the RETRAN no-slip or homogeneous-equilibrium-model (HEM) option). These figures are meant only to provide an indication of the sensitivity of the dependent quantiles relative to their respective input parameter of principal influence. They do not provide an exact correlation since more than one input parameter may have been changed between points on each graph; this results from an attempt to hasten the seatch for a reasonable steady state by simultaneous changing of several input parameters. The horizontal dashed line across each of these three figures represents the desired value of the

dependent variables (full power values).

In the reference study (reference 1), two-phase mixtures were modeled using RETRAN's homogeneous equilibrium model (HEM). During this study, a dynamic slip model for two phase mixtures became available, and its utilization was expected to have a strong influence on junction 23 and 63 loss coefficients calculated during steady state initialization. A switch to the dynamic slip option was made with the following consequences being noticed: at full power, the loss coefficients calculated by RETRAN at junctions 23 and 63 did not change noticeably at a given recirculation ratio (3.25), but the loss coefficients decreased substantially at four percent power for a given recirculation ratio (40). This required the decrease of the four percent power recirculation ratio (relative to the HEM case) so that the calculate junction 23 and 63 loss coefficients would approach the 100 percent power values. An explanation for the change of loss coefficient only at four percent power, when switching to the dynamic slip option is as follows:

1) The dynamic slip option allows the vapor phase to move faster than the liquid phase where the HEM option does not.
2) Since the vapor moves faster when using the dynamic slip option, it comprises less of the cross-sectional area in the tube region than when the HEM option is used; thus, the density of the fluid is greater and does not change as rapidly with increasing elevation with the dynamic slip option.
3) Thus the driving force behind the circulation of steam generator flow, the lower average value of fluid density in the tube region, is decreased when using the dynamic slip option.
4) However, this decrease of driving force is almost completely offset by a decrease of two phase friction in the tube region at 100 percent power, and consequently the natural circulation rate is not affected significantly. At low power the slip model also reduces

the void fraction and thus brings about compensating changes in buoancy and two phase friction. However, since the void fraction at low power is much smaller than at high power, the reduction of two phase friction is less, and the change in buoancy must be compensated by a reduction in flow rate (recirculation ratio).

Table 3 lists values for the input parameters varied and their corresponding dependent quantities at full power and at four percent power as used for the remainder of this study (except as in appendix I). The listed four percent power steam carry-under of 1.8 percent is somewhat higher than the maximum suggested value of 0.5 percent. Further adjustment of the enthalpy of volumes 31 and 71 in order to obtain a lower carry-under is not necessary here since it will not affect results noticeably (compare with appendix I). The values of junctions 68 and 28 loss coefficients at 4 percent power are approximately 5 times their respective values at 100 percent power. This is not unreasonable because of the extreme sensitivity of these variables to the liquid livels in volumes 67 and 27 (see Fig. 5): less than one tenth of an inch variation of volume 67 and 27 liquid levels accounts for the discrepancy between listed four percent and full power values of junction 68 and 28 loss coefficients. The actual liquid level in the steam generator is not known to this degree of accuracy at any power level.

Other dependent quantities listed in table 3 also do not give exact agreement between the 4 and 100 percent power cases, but these discrepancies too will not have strong effects on conditions of interest during the steam line break.

Input Parameter Varied	Dependent Variable
Recirculation Ratio	Junctions 63 & 23 Loss Coefficients
Volumes 27 & 67 Liquid Level	Junctions 68 & 28 Loss Coefficients
Volumes 31 & 71 Enthalpy	Steam Carry-under
Volume 9 Enthalpy	Calculated Heat Transfer Area

Table 2. Input Parameters Varied and their Corresponding Major Dependent Variables.

Dependent Variable/ Independent Parameter	Full Power Value	Four Percent Power Value
Junction 63 Loss Coefficient / Recirculation Ratio	149.5 / 3.25	197.5 / 40.0
Junction 23 Loss Coefficient / Recirculation Ratio	150.0 / 3.25	198.0 / 40.0
Junction 68 Loss Coefficient / Vol. 67 Liquid Level	7.55 / 3.5	40.7 / 2.64
Junction 28 Loss Coefficient / Vol. 27 Liquid Level	7.54 / 3.5	40.6 / 2.64
Steam Carry-under (percent) / Vol. 31 (and 71) Enthalpy (BTU/lbm)	0.45 / 550.5	1.8 / 553.26
Calculated Heat Transfer Area Percent Difference / Volume 9 Enthalpy (BTU/lbm)	3.7 / 550.2	1.9 / 559.4

Table 3. Values of Independent Parameters Used and the Resulting Dependent Parameters Calculated in Steady State Initialization

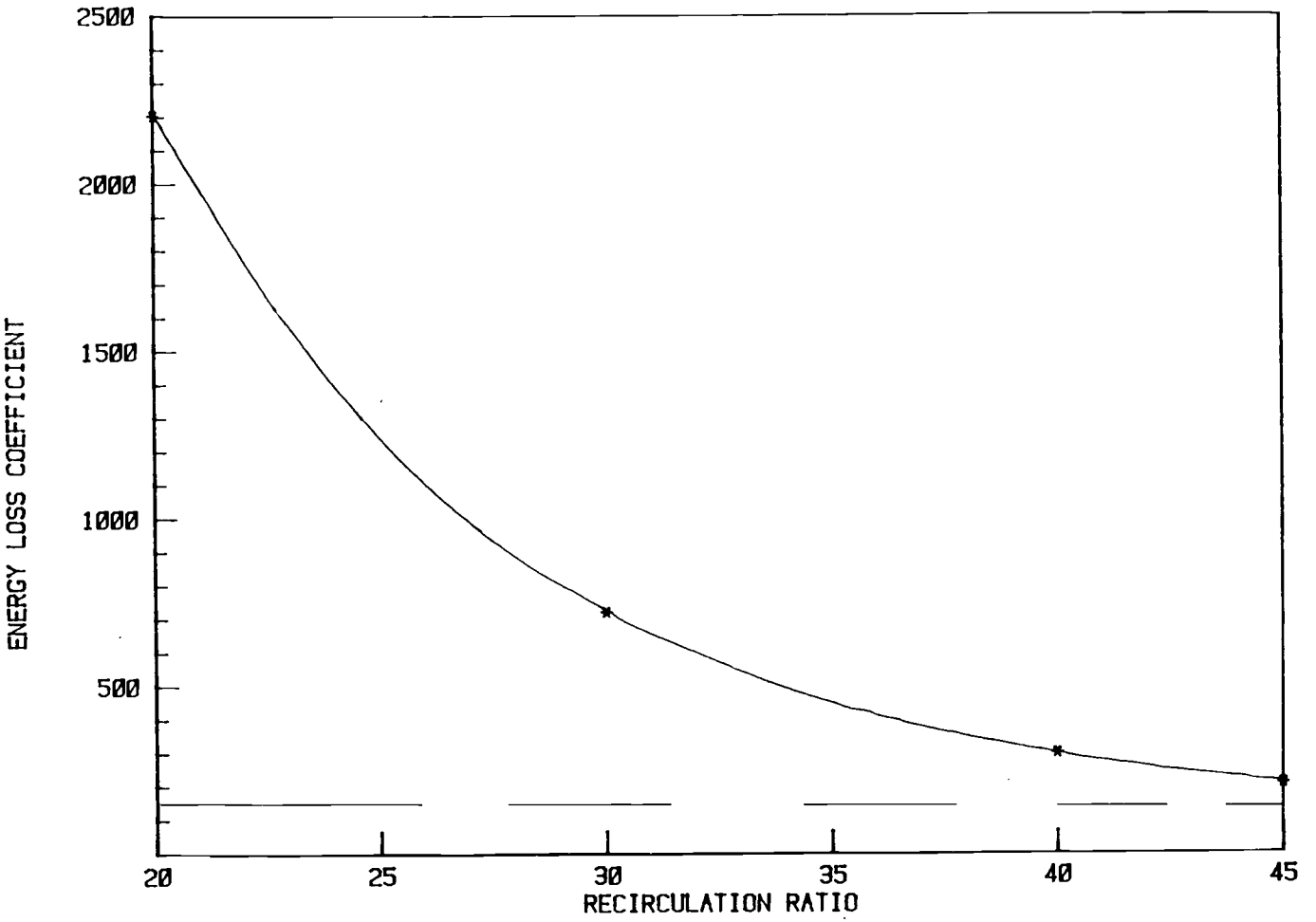

Fig. 5 Junction 63 and 23 Loss Coefficient Vs. Recirculation Ratio

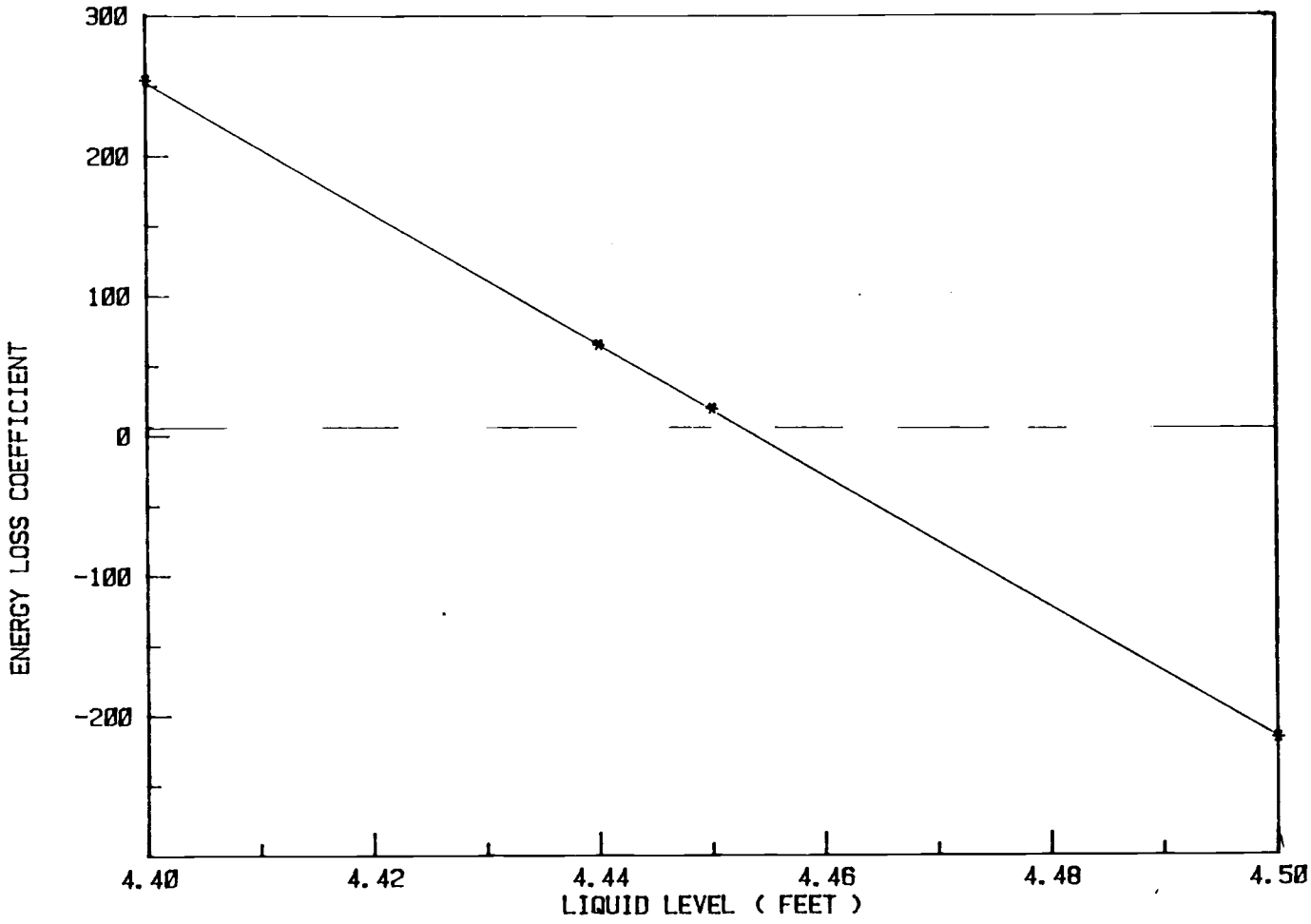

Fig. 6 Junction 68 (and 28) Loss Coefficient Vs. Volume 67 (and 27) Liquid Level

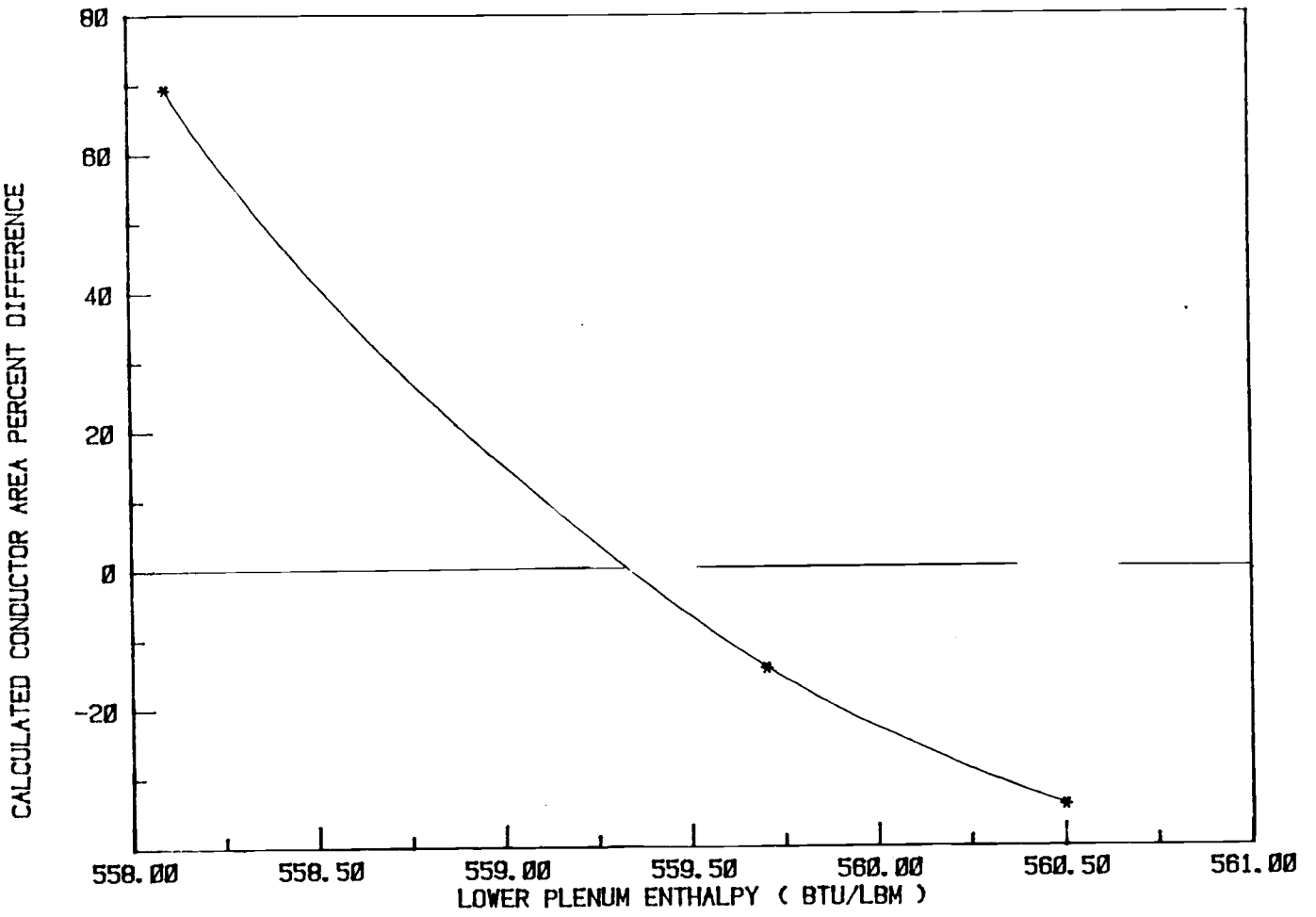

Fig. 7 Calculated Conductor Area Percent Difference From Input Value Vs. Lower Plenum Enthalpy

4. The Steam Line Break Model

Fig. 8 shows the atual geometry in the direct vicinity of the steam line break, which is assumed to occur at the steam line weld within the primary containment penetration region. This weld is chosen as the break site because welds in general are potential weak spots and because this weld is located where inspection and maintenance are difficult.

Modeling a guillotine break with RETRAN poses the problem of describing the pipe separation phenomenon after the break. As the broken ends pull away from each other, steam will flow from each end into the region surrounding the break. However, during the initial phase of the break there will be some interaction of the fluid streams emerging from the broken ends due to incomplete dislocation. Path 2 (see below) represents this interaction.

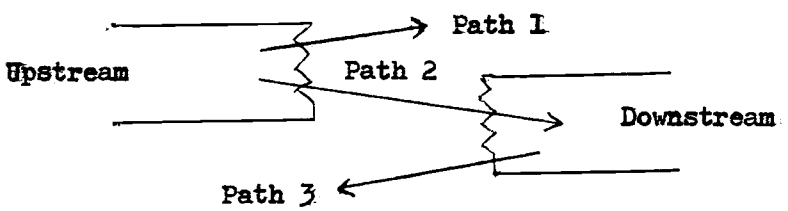

Thus, three flow paths will occur during the transient, and these are modeled in this study as (fictitious) valves. With the pipe intact, only one flow path exists (path 2), implying that its representative valve is fully open while the others are fully closed. After the entire break action, with no flow between the broken ends, flow paths 1 and 3 are fully open while flow path 2 is closed.

A one valve model is inadequate since it can only represent a hole in the pipe wall. A two valve model is also inappropriate since it can only represent either two holes or one hole accompanied by a flow blockage.

The area associated with the break flow paths can be

prescribed as a function of time through each path's representative valve. This brings up an important problem: as the broken pipe ends separate, what areas should be associated with each valve? If the broken ends remain overlapped as shown below,

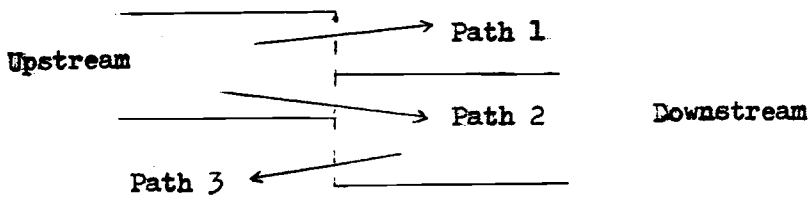

it is natural to have equal areas for paths 1 and 3, and the sum of paths 1 and 2 areas equal to the original pipe area. However, if the broken ends should separate, the areas to associate with each flow path are not as obvious. For example, how far apart would the two ends have to be before flow path 2 closes completely if pipe separation was only in the axial direction, and what portion of the open area between the ends would be appropriate for each of flow paths 1 and 3 during the separation?

For a simple guillotine break outside of the penetration region, a conservative break scenario (relative to mass and energy release rates) is to assume a linear change in all flow path areas with a total opening/closing time of one millisecond; however, when the presence of the penetration region around the break is considered, this opening/closing rate may be overly conservative. This is because the sleeve of the penetration region restricts the downstream piping section (which is free to move) to a 7.69 inch lateral displacement, which cannot independently close flow path 2. Thus, to stop all flow between the broken ends, the downstream section must pull away horizontally from the upstream section, requiring the acceleration and movement of a heavy section of pipe. Estimation of this movement will result in an estimate of pipe separation.

To show more fully the possible results of the pipe rupture, five break area ramps were used for paths 1, 2, and 3 (valves 800,

249, and 801 respectively): a one millisecond linear ramp, and a break ramp as listed in Table 4 with the time values multiplied by 1 of 4 constants (0.5, 0.75, 1.0, 1.25) for each run. Table 4 is a list of data for a likely break scenario developed by PGE.

Including the annular penetration region in the model (steam line break model 2 - Fig. 9) reduces the transient severity relative to modeling without the annular region (steam line break model 1 - Fig. 10) since the annulus maintains a pressure approximately 200 psi higher than the environment outside of it and serves to restrict flow from the ruptured pipe. Fig. 11 shows the total mass flow rate for break model 2 with all 5 break valve area ramps. The one millisecond linear ramp is unrealistically quick considering that the break occurs within the penetration annulus, but it does serve as a limiting case for the rapidity of the break: the actual break rate will be slower and the resulting maximum mass and energy release rates will be lower. This cannot be said without some doubt relative to the other 4 break valve area ramps. Table 4 lists estimates of the break valve areas based on the maximum thrust from the downstream section and its resistance to movement. Although the thrust provides an estimate of the separation between broken ends as the break progresses, it still requires the additional estimation of break valve areas (which would be uncertain even if the relative positions of the broken ends were known exactly). Thus, a break rate faster than that of Table 4 may be required to ensure conservative results. Fig. 12 covers the first 0.4 seconds of Fig. 11 on a linear time scale for ease of comparison between curves. It indicates little variation in severity of break flow rates: the main difference is that the peaks are shifted with respect to time. Thus, little conservatism is gained by assuming much quicker opening rates than that of Table 4.

Figures 13 and 14 show the steam line break mass flow rate, enthalpy, and quality (at junction 803) for break model 2 with a one millisecond break ramp and a break as in Table 4.

Time (sec)	Junctions 800 & 801 Normalized Area	Junction 249 Normalized Area
0.0	0.0	1.0
0.001	0.0768	0.9232
0.011	0.0806	0.9194
0.021	0.0885	0.9115
0.027	0.0962	0.9038
0.031	0.1062	0.8974
0.041	0.1231	0.8769
0.051	0.1515	0.8485
0.061	0.1895	0.8105
0.071	0.2397	0.7603
0.081	0.3051	0.6949
0.091	0.3901	0.6099
0.101	0.5001	0.4999
0.111	0.6421	0.3579
0.122	0.8457	0.1543
0.131	0.8914	0.1086
0.141	0.9337	0.0663
0.151	0.9669	0.0331
0.161	1.0	0.0
2.0	1.0	0.0

Table 4. Normalized Steam Line Break Valve Area Vs. Time

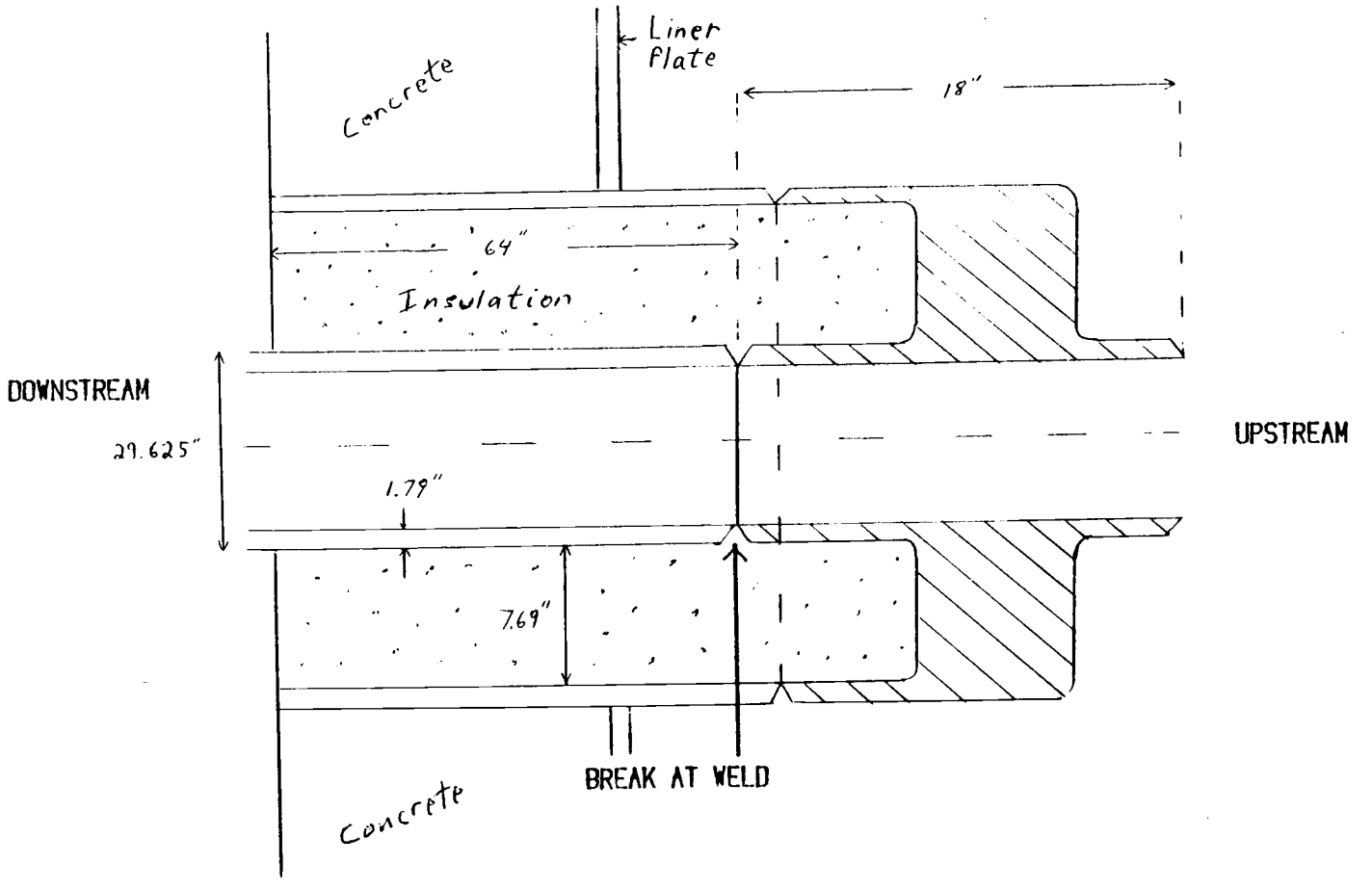

Fig. 8 Primary Containment Penetration Region

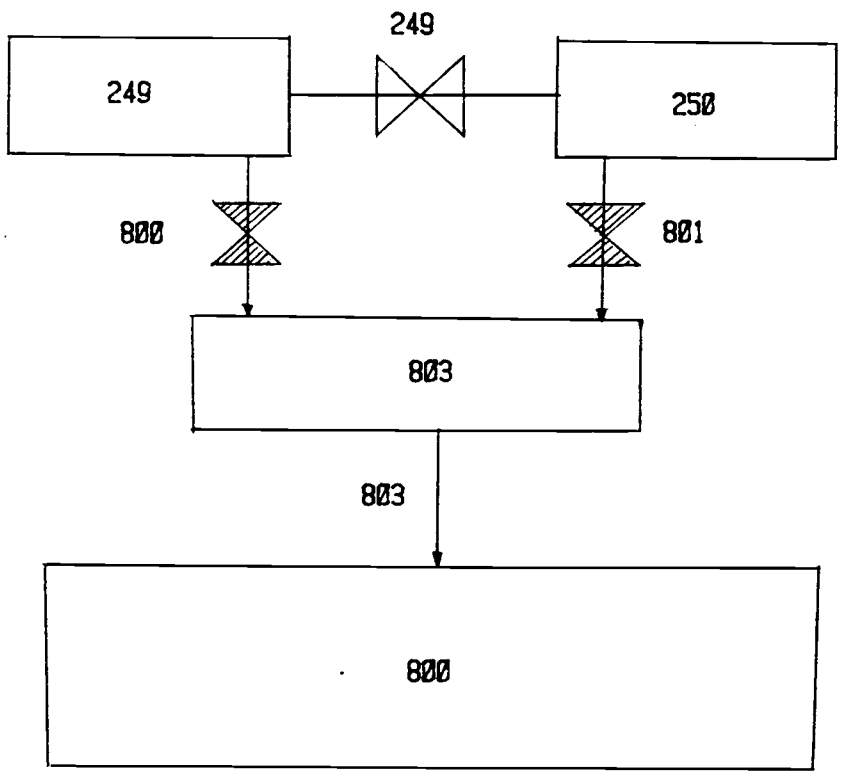

Fig. 9 Steam Line Break Model 2

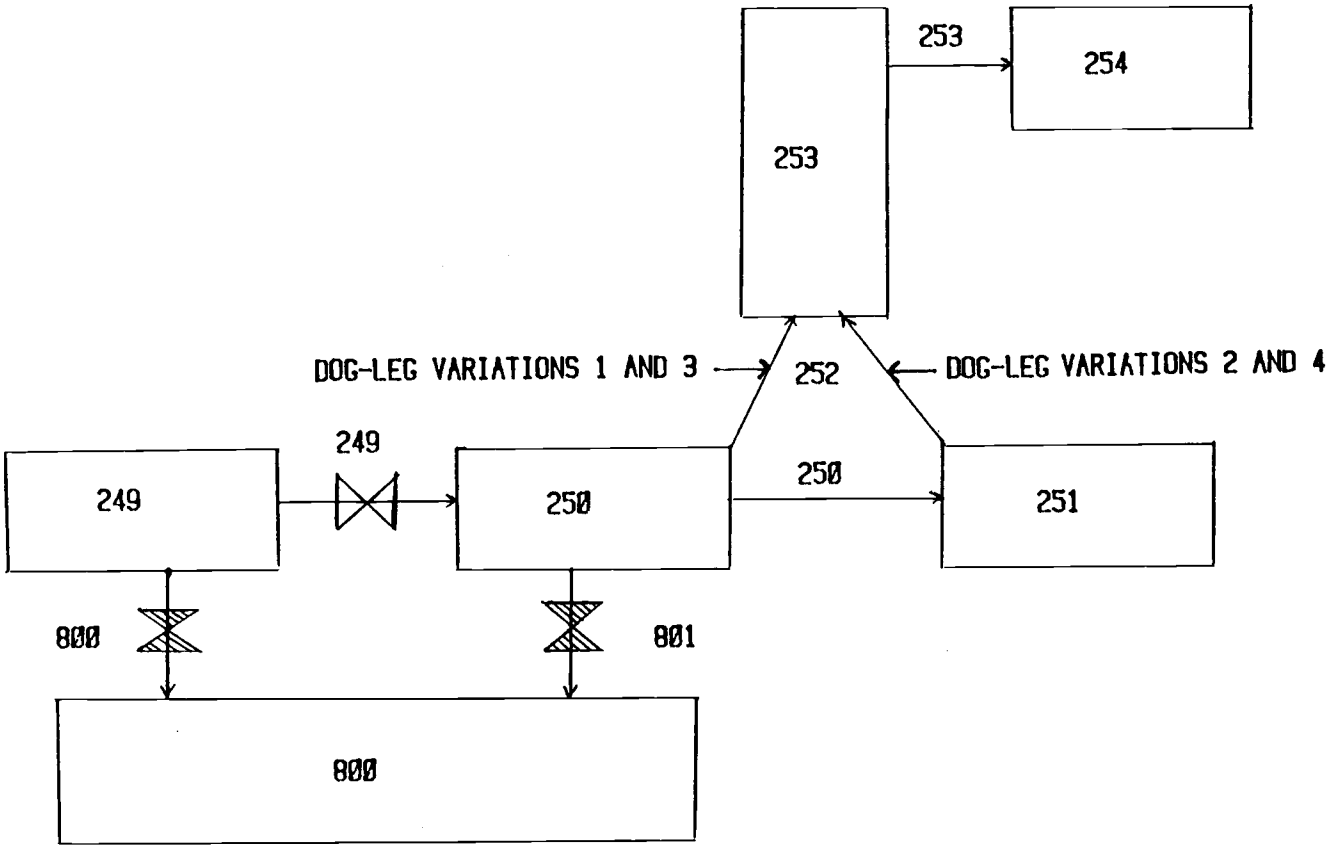

Fig. 10 Steam Line Break Model 1 With Relief Valve Header (Dog-leg) Variation Positions

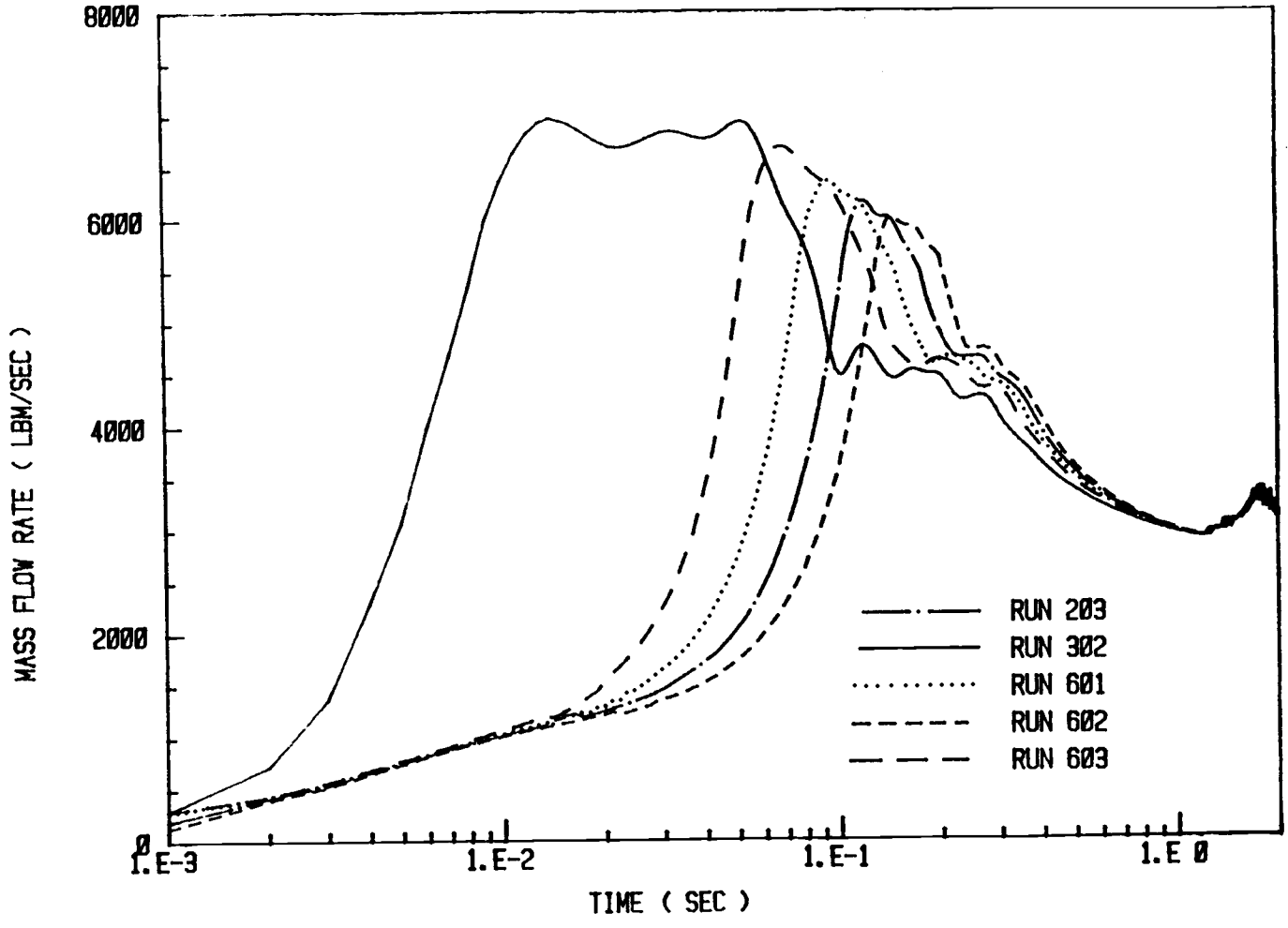

Fig. 11 Break Rate Sensitivity for Break Model 2

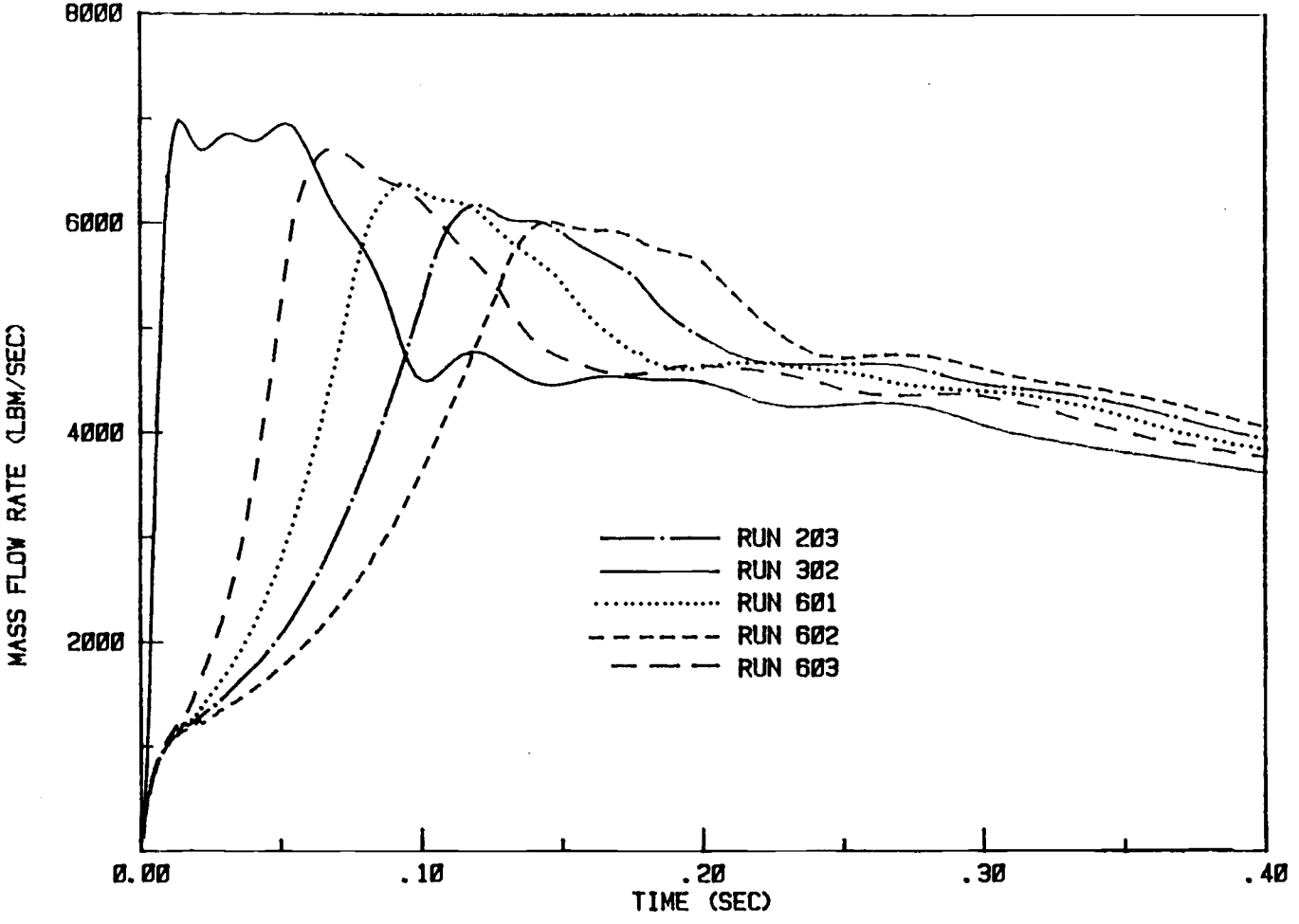

Fig. 12 Break Rate Sensitivity for Break Model 2 (First 0.4 sec.)

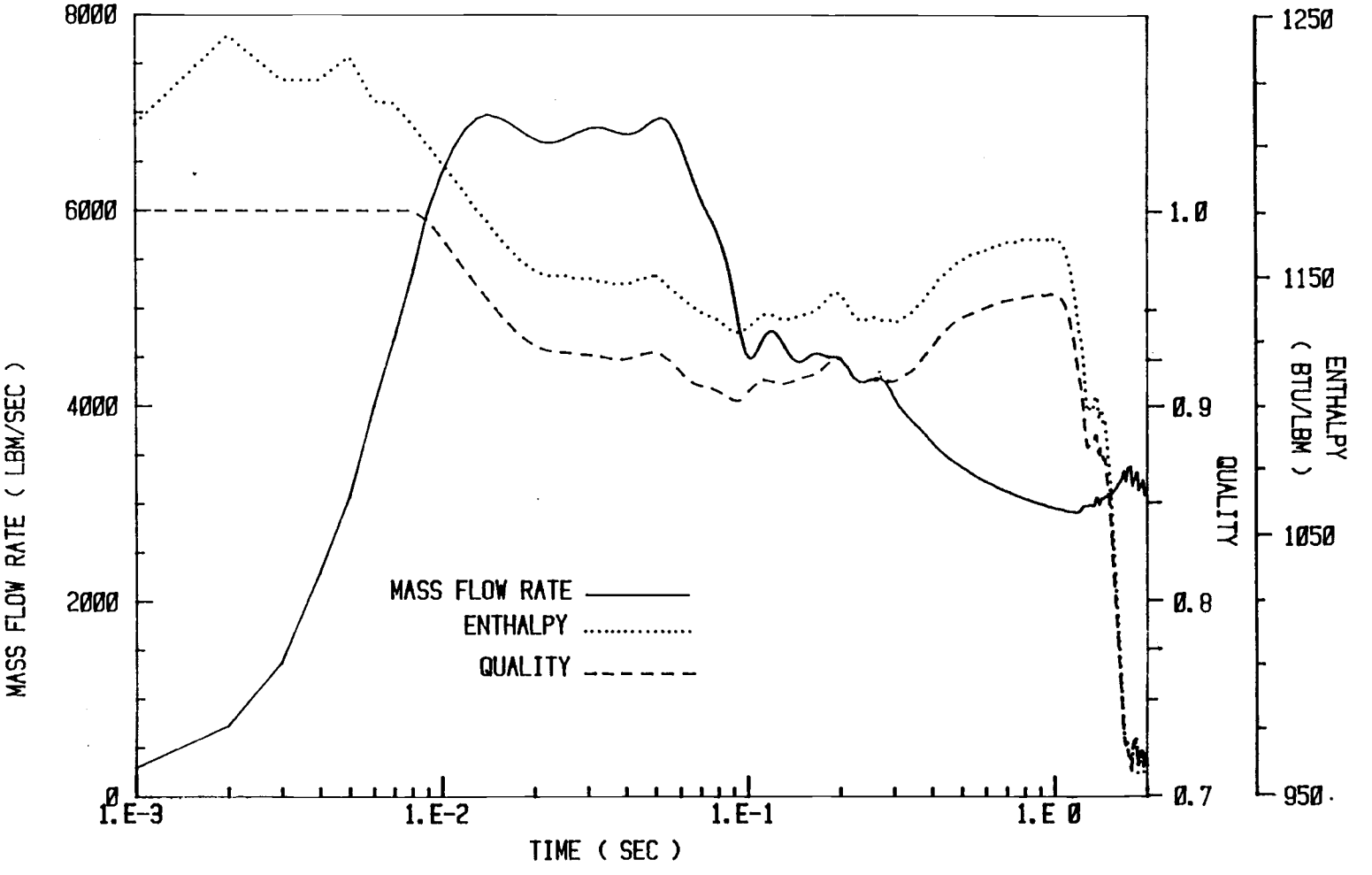

Fig. 13 Junction 803 Mass Flow Rate, Enthalpy, and Quality for Run 302 (One Millisecond Break)

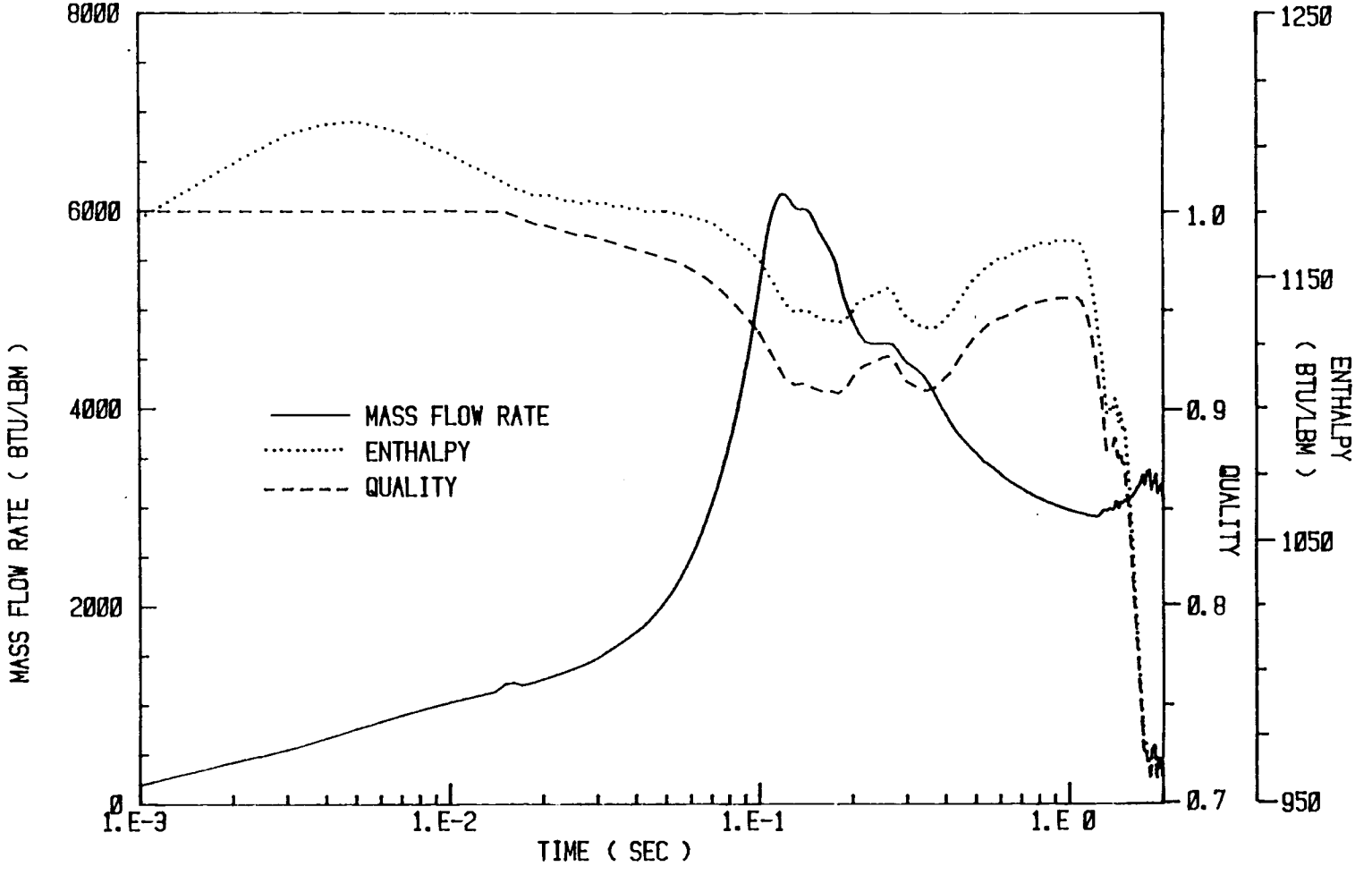

Fig. 14 Junction 803 Mass Flow Rate, Enthalpy, and Quality for Run 203 (Break as in Table 4)

4.1 Modeling Variations and Justifications

To explore the sensitivity of the results to various modeling assumptions, several variations in modeling were studied.

Steam line break model 1 (Fig. 10) models the rupture without consideration of the presence of the annular penetration region (volume 803). Fig. 15 shows the total break mass flow rate for all five break valve area ramps, and Fig. 15A covers the first 0.4 seconds of Fig. 15 on a linear time scale for ease of comparison. Comparison of figures 11 and 12 with figures 15 and 15A respectively indictes that break model 1 yields higher flow rates for each break ramp. Should a pipe rupture actually accur outside of the penetration region, break model 1 with a one millisecond break ramp provides an adequately conservative estimate of the actual behavior; the other four break ramps do not apply well in this case, but were included for the purpose of comparison.

Critical flow at junctions 240 (venturi), 249, 800, 801, and 803 (when present) was modeled by the isoenthalpic expansion model provided by RETRAN. For each time step, flow at each junction where choked flow conditions are expected is calculated using both the inertial and choking models, and the larger value is rejected. When choking occurs, the RETRAN solution becomes uncoupled at the choked junction: the junction flow conditions are a function of the upstream fluid conditions only. Thus, variations in modeling techniques and perturbations introduced downstream of a junction experiencing critical flow can not affect that junction as long as critical flow prevails. This fact justifies the modeling of the environment surrounding the pipe rupture by an infinite (constant) volume (volume 800) filled with saturated steam at atmospheric pressure. The actual pressure of the environment surrounding the break will not be high enough to stop critical flow at junction 800

(upstream break junction) for break model 1, or junction 803 (penetration exit juncion) for break model 2. However, for break model 1, as the transient progresses and the downstream section evacuates, choking at junction 801 (downstream break junction) will stop at some time; since the actual pressure surrounding the rupture at this time will be greater than the constant value of 14.7 psi assigned to volume 800, the actual time when choking ceases could only be earlier and the actual evacuation of the downstream section could only be less complete than the results with the assumption used in the model. Thus, the infinite volume representing the surroundings is slightly conservative with respect to flow rates only through junction 801 when using break model 1.

In break model 2, critical flow models were used in junction 800 and 801 (entrance junctions to the penetration region) for the following reasons:

1) An area change occurs at both junctions 800 and 801.
2) The flow rate at junction 800 was noticeably higher for break model 2 without choking at junction 800 than for break model 1 (see Fig. 16).
3) Smooth results were obtained when choking was allowed at junctions 800 and 801: these junctions did not experience unreasonable oscillation between choked and unchoked conditions

In addition to the isoenthalpic expansion model provided by RETRAN, the code offers other critical flow models. Figures 17 and 18 indicate results using no choking, Moody, and isoenthalpic expansion critical flow models for comparison. The no choking model yields extremely high flow rates as expected. The Moody choking model yields slightly higher results than the isoenthalpic expansion model, which was anticipated (see reference 3); however, no mention of the applicability of the Moody model above 400 psi is made in reference 3. The isoenthalpic expansion model is reportedly quite accurate (see reference 3) at the pressures encountered during this transient.

For the slower steam line break rates another complication

arose for both break models when critical flow was not allowed in junction 249 (interaction junction between broken pipe ends): the code suffered an apparent convergence problem and terminated execution due to negative enthalpy at junction 249, which it encountered during its search (which was unsuccessful) for a converged solution. Upon examination of the output, a specific mass flow rate of 15000 lbm/sec-ft^2 at junction 249 was found. This is unreasonable since the specific mass flow rate for junction 800 for any of the runs in this study was less than 2000 lbm/sec-ft^2 : since volume 249 was directly upstream of junctions 249 and 800 when execution terminated, the maximum specific flow rate possible at junction 249 is that of junction 800 (which is less than 2000 lbm/sec-ft^2), where critical flow occurs. Thus, a critical flow model for junction 249 appeared to be necessary, and its implementation eliminated the associated complication. Fig. 19 indicates junction 249 mass flow rates with and without the modeling of critical flow, and junction 249 normalized area (using a break as in Table 4). The mass flow rates for both cases agree closely until choking is seen in one, where a decrease of mass flow rate dictated by the closing valve is observed; meanwhile, the mass flow rate of the unchoked case continues to increase and eventually results in run termination. For cases with a one millisecond break, valve 249 closed so fast that associated solution problems did not occur.

Both break models use 1.0 for the choked flow contraction coefficients. since the contraction coefficient multipied by the junction area gives the effective cross sectional area at the throat of the critical flow region, the contraction coefficient used is conservative, yielding flow and energy release rates larger than expected.

Various system paramters had to be estimated for input to the RETRAN model. The loss coefficients for junctions 800, 801 (both break models), and 803 (break model 2) were assigned the value 1.0, which is a typical value for an abrupt opening into a large area. Figures 20 and 21 compare mass flow rates at junctions 800 and 801

for various loss coefficients using break model 1 with a one millisecond break ramp. Although the actual loss coefficients are not exactly 1.0, they are probably much closer to this value than the bracketing values of 0.25 and 4.0 used to develop figures 20 and 21.

The junction inertias for junctions 800 and 801 were calculated as 0.5(L/A) of volumes 249 and 250 respectively when using break model 1 (L=volume length, A=volume area). The junction inertia (I) for a section of a straight pipe is defined as 0.5(Lu/Au + Ld/Ad) where u and d refer to the volume immediately upstream and downstream from the junction respectively. For a flow path other than a straight pipe, it may be desirable to use a value for the junction inertia which differs from that defined above. Since L/A for an infinite volume is zero, the input junction 800 and 801 inertias appear reasonable. Fig. 22 demonstrates the effects of altering the break junction inertias for break model 1. For a given set of conditions on either side of a junction, acceleration of flow through the junction is inversely proportional to the junction inertia. Thus, the larger inertia yields slightly lower peaks and slightly lags the results using smaller inertias (similar to the effect seen with altered junction loss coefficients). Although neither junction inertias or loss coefficients are used when critical flow occurs, they do affect results prior to choking and also affect the point in time when choking occurs.

For break model 2 the inertias of junctions 800 and 801 were computed as defined above, while the inertia for junction 803 was calculated as 0.5(L/A) of volume 803 (the reasoning being the same as above).

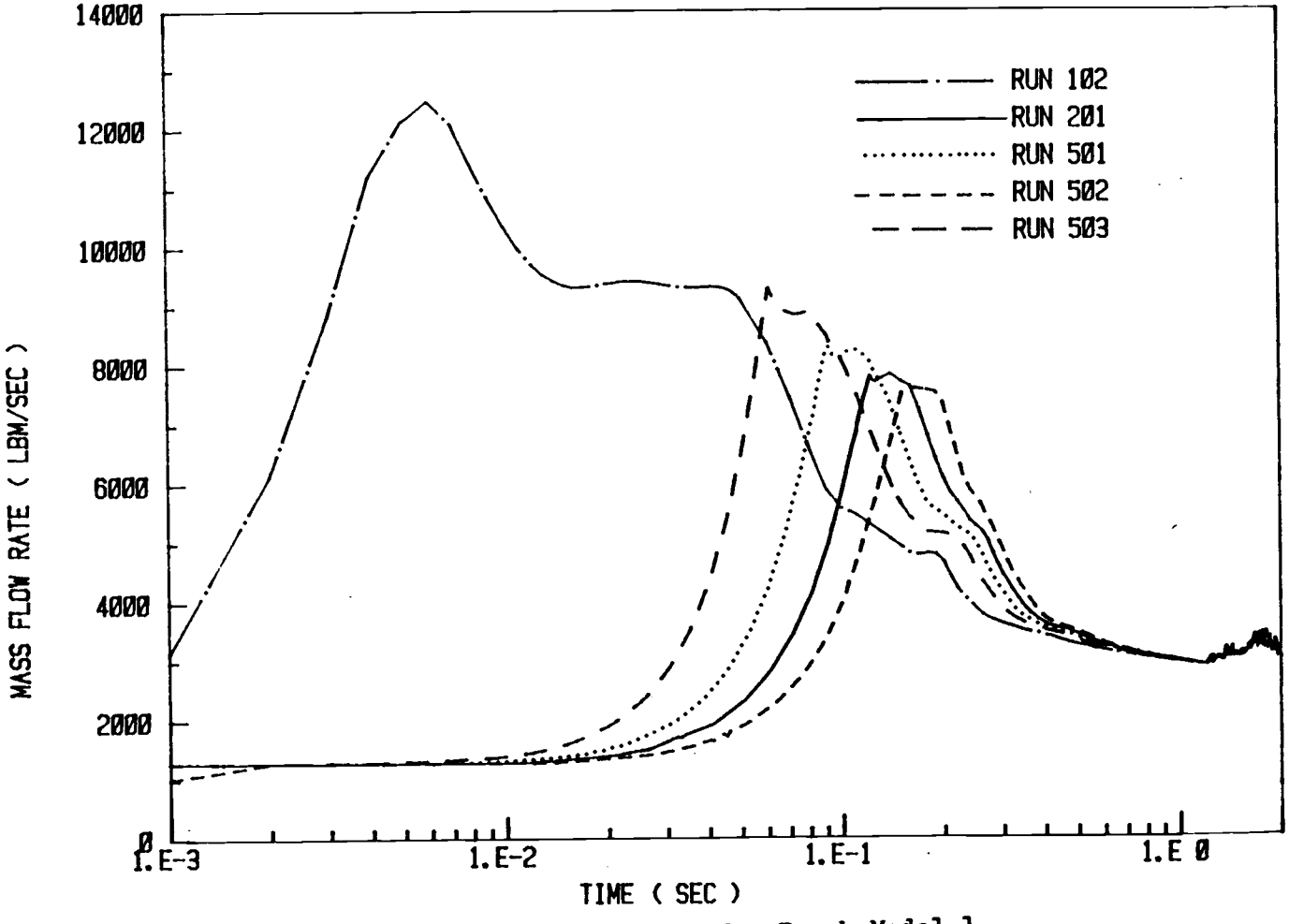

Fig. 15 Break Rate Sensitivity for Break Model 1

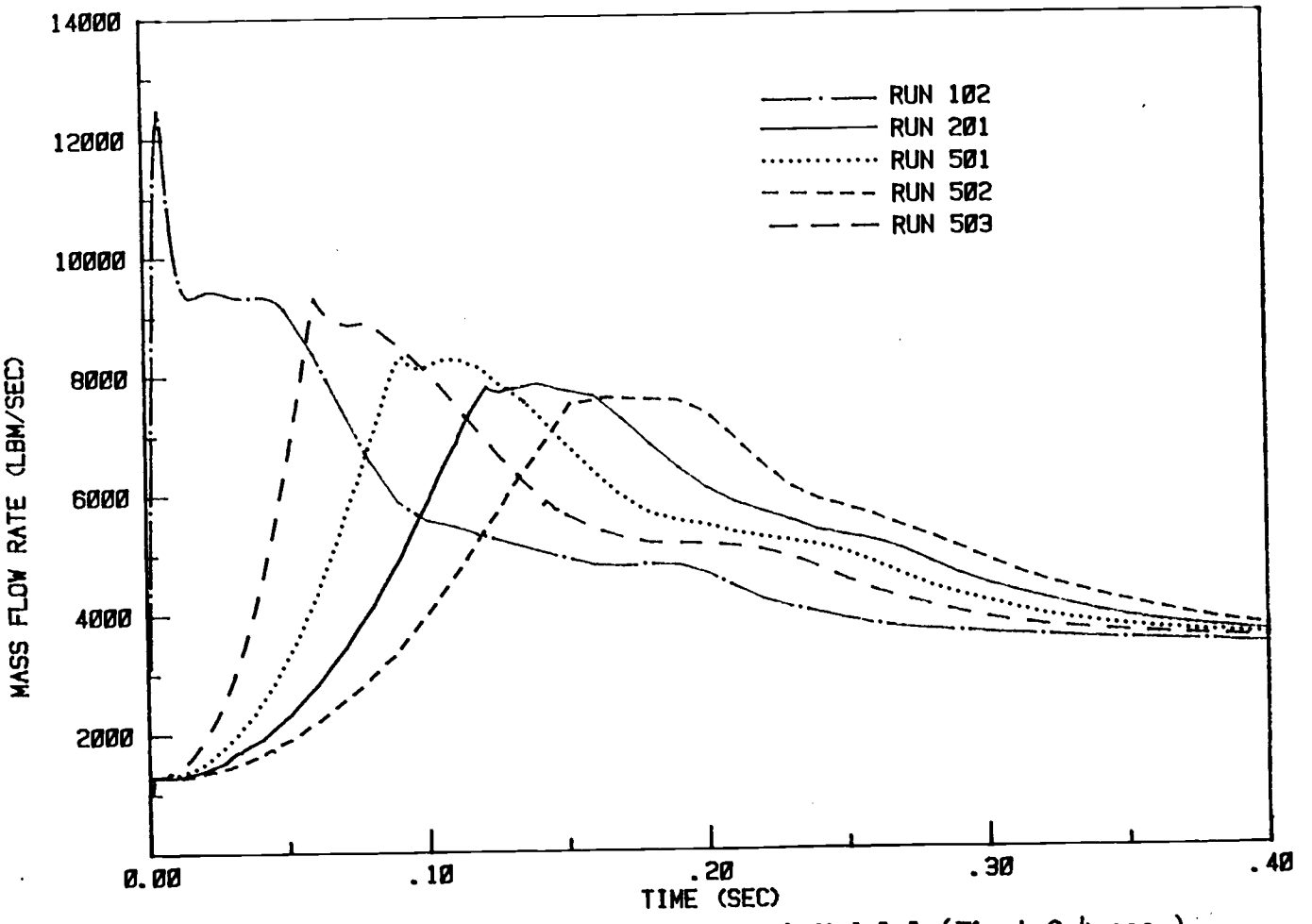

Fig. 15A Break Rate Sensitivity for Break Model 1 (First 0.4 sec.)

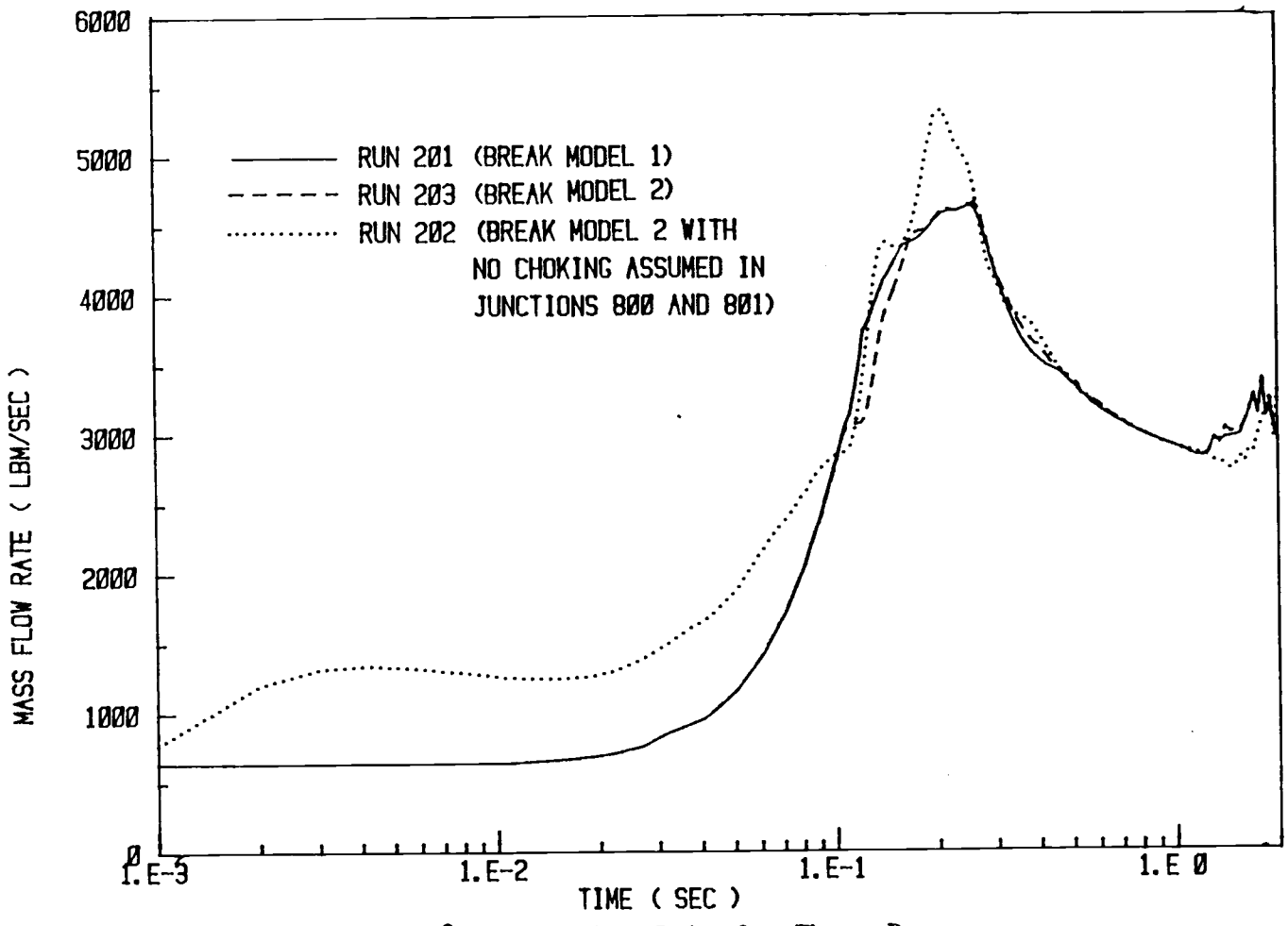

Fig. 16 Junction 800 Mass Flow Rate for Three Runs (Break as Listed in Table 4)

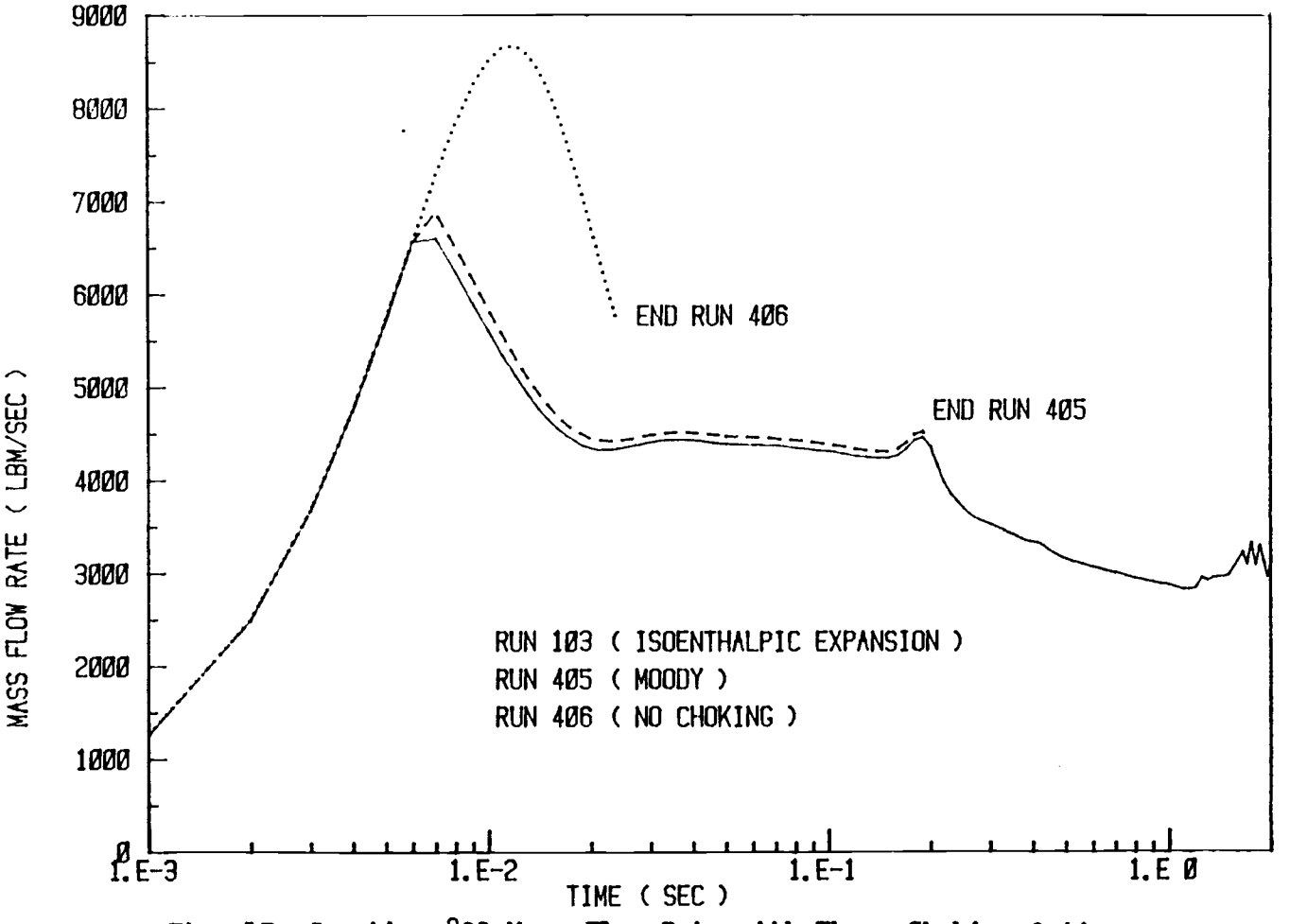

Fig. 17 Junction 800 Mass Flow Rate with Three Choking Options (One Millisecond Break)

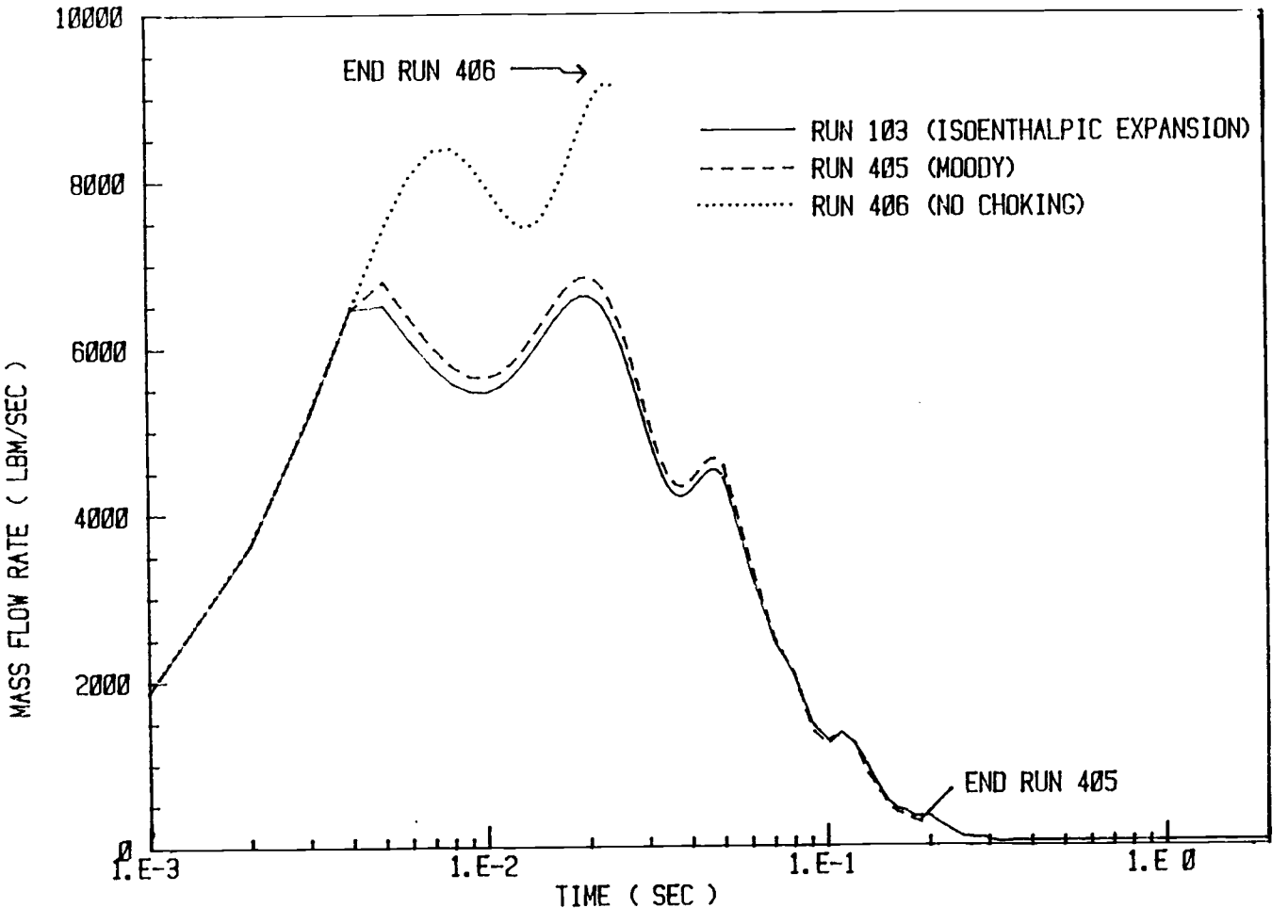

Fig. 18 Junction 801 Mass Flow Rate with Three Choking Options (One Millisecond Break)

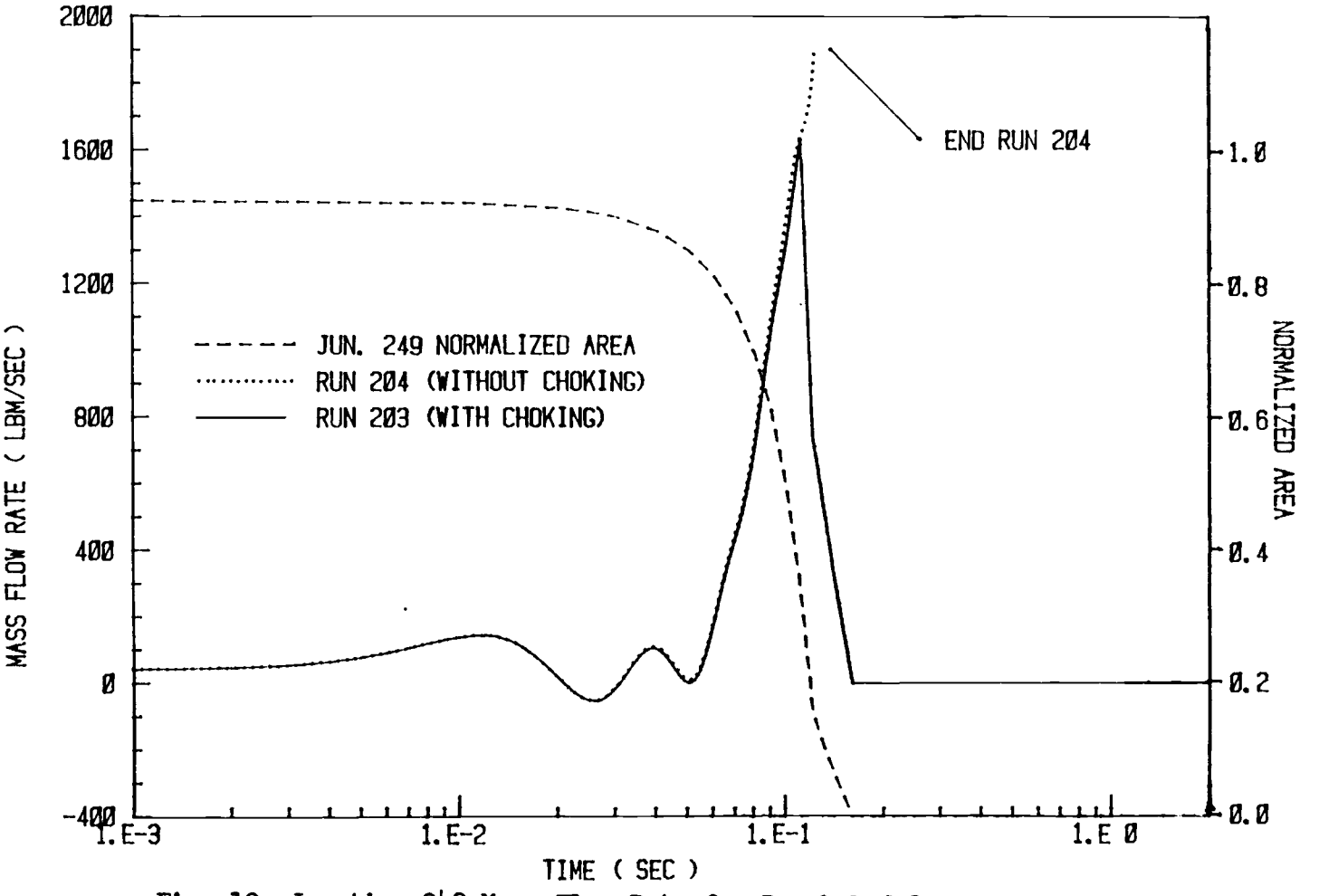

Fig. 19 Junction 249 Mass Flow Rate for Break Model 2 with and without Choking in Junction 249 (Table 4 Normalized Break Area is Shown)

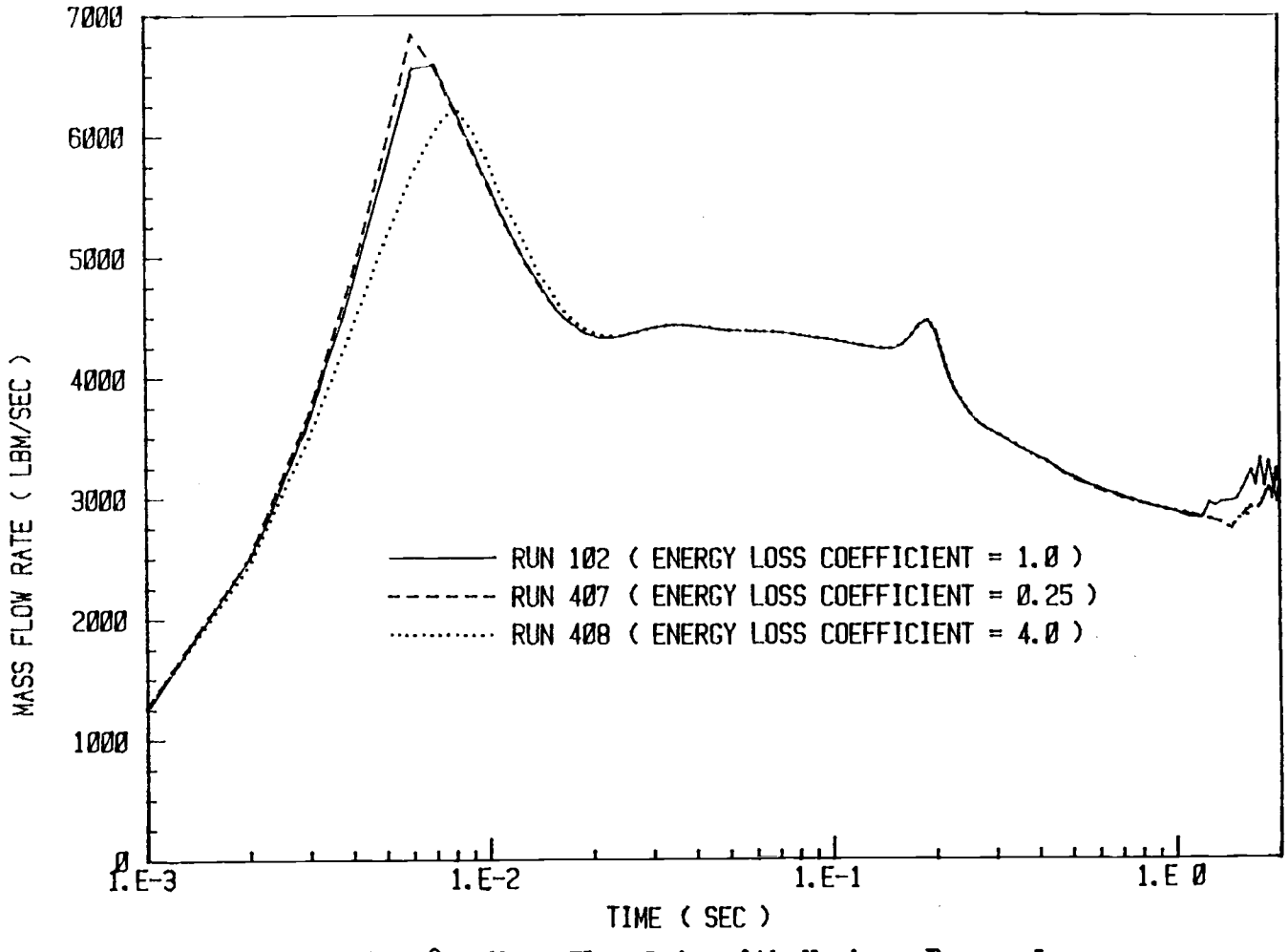

Fig. 20 Junction 800 Mass Flow Rate with Various Energy Loss Coefficients for Junction 800

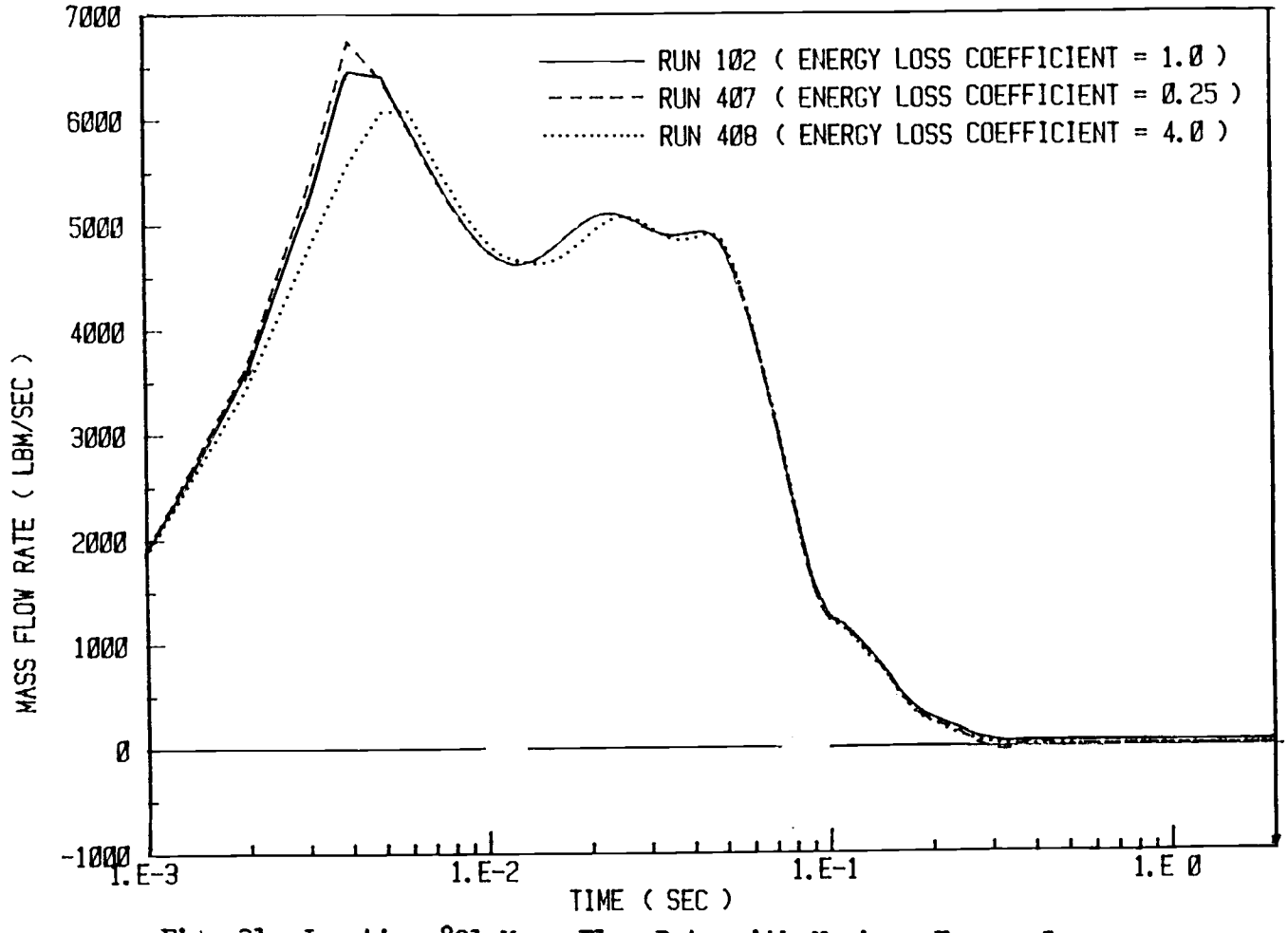

Fig. 21 Junction 801 Mass Flow Rate with Various Energy Loss Coefficients for Junction 801

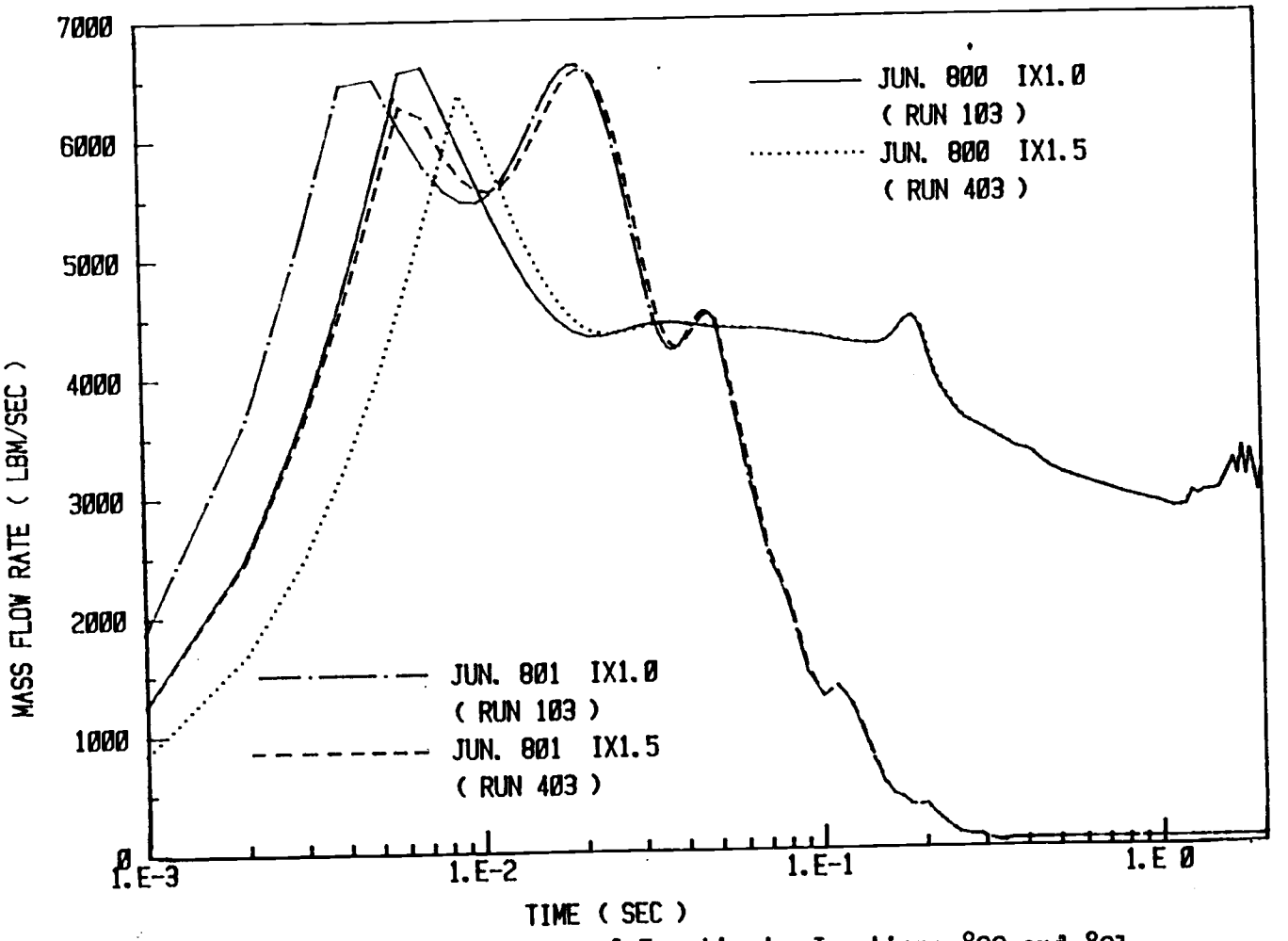

Fig. 22 Effects of Increased Inertia in Junctions 800 and 801

4.2 Variations in Downstream Section Modeling

Fig. 10 also depicts the region downstream from the break, which proved troublesome during transients with fast break valve opening rates using break model 1: the code sometimes encountered negative mass or energies in this region as it searched for a converged solution. For break model 1, separation of piping sections upstream and downstream from the break occurs once valve 249 closes due to the presence of infinite (constant) volume 800. Since the total break time was 0.001 sec and steam line break model 1 was being used when the above errors occurred, it appeared that a change in the section downstream from the break was required. Thus, a search was made for a modeling technique in the downstream region which would independently eliminate run termination due to instabilities in this region.

In a model with low resolution (coarse nodalization), the behavior of the pressure waves introduced into the system by opening and closing valves can be altered significantly by making modest geometric alterations (changing the nodalization) or by changing the constitutive equations. Alteration of pressure wave reflection and propogation in many cases might result in significant changes in the shape of transient response functions because of altered superposition of waves and their reflections. By developing variations in the model, it was hoped that transient reponses resulting in termination could be avoided.

The sensitivity studies regarding nodalization may concern volume nodes as well as connecting junctions relative to each other. Of particular concern here was the connection of the relief valve header (dog-leg) volumes (volumes 253 and 254) to the steam line as shown in Fig. 10: volume 253 is attached either to volume 250 or 251. Although moving the dog-leg junction 252 may seem artificial, its actual position falls on the junction between volumes 250 and 251, so it can be associated with either of these volumes.

Another change in nodalization was made by varying the number of volumes in the downstream region. Volume 259 was divided into two equal volumes in one instance, and all four of the downstream volumes were divided into two equal volumes in another instance.

One method of changing the constitutive equations is to include the vectoral nature of the momentum equation at junction 252 by specifying the input parameter ANGLJ=90 degrees, which indicates that the flow paths in the volumes joined by junction 252 are perpendicular. When using ANGLJ=0 degrees (as in the reference case), the momentum equation reduces to a one dimensional form (as would be used for a straight pipe).

Another method of changing the constitutive momentum equation is to use the no momentum mixing option (MVMIX=3) available in RETRAN (in contrast to the compressible flow single stream option) at junction 252, which removes the momentum flux terms due to compressibility and area changes. The result is a model for a Tee without consideration of the momentum flux components of the momentum equation (equation 2 below). The compressible flow single stream option (MVMIX=0) with ANGLJ=0 degrees implies a one dimensional momentum equation formulation: all flow is assumed to occur along a straight line (equation 1 below). The compressible flow single stream and the no momentum mixing equations used in RETRAN take on the forms (respectively):

$$1)\quad \frac{1}{2}\left[\frac{L_k}{A_k}+\frac{L_{k+1}}{A_{k+1}}\right]\frac{dW_i}{dt}=\frac{\bar{W}_k^2}{\bar{\rho}_k A_k^2}-\frac{\bar{W}_{k+1}^2}{\bar{\rho}_{k+1} A_{k+1}^2}+p_k-p_{k+1}-\frac{1}{A_k}F_{w,k}$$

$$-\frac{1}{A_{k+1}}F_{w,k+1}-\frac{1}{A_k}\bar{M}\,\frac{1}{2}V_k\,g_{z,k}-\frac{1}{A_{k+1}}\bar{M}\,\frac{1}{2}V_{k+1}\,g_{z,k+1}$$

$$+\frac{W_i^2}{2\rho_i}\left[\frac{1}{A_{k+1}^2}-\frac{1}{A_k^2}\right]-\frac{W_i|W_i|\dot{e}_v}{\rho_i A_i^2}$$

$$2)\quad \frac{1}{2}\left[\frac{L_k}{A_k}+\frac{L_{k+1}}{A_{k+1}}\right]\frac{dW_i}{dt}=p_k-p_{k+1}-\frac{1}{A_k}F_{w,k}-\frac{1}{A_{k+1}}F_{w,k+1}$$

$$-\frac{1}{A_k}\bar{M}\,\frac{1}{2}V_k\,g_{z,k}-\frac{1}{A_{k+1}}\bar{M}\,\frac{1}{2}V_{k+1}\,g_{z,k+1}-\frac{W_i|W_i|\dot{e}_v}{\rho_i A_i^2}$$

were the subscript i refers to the junction separating volumes k

and k+1, L=volume length, A=volume area, W=junction mass flow rate, p=volume pressure (at center), F_w=wall friction term in a volume, $\bar{M}_{\frac{1}{2}V}$=the mass in one half of a volume, g_z=gravitational constant, ρ_i = junction density, and e_v^* is an irreversible junction loss coefficient.

Table 5 lists the variations and indicates those which were successful (i.e. which ran the entire 2 seconds).

Using the no momentum mixing option corresponds to the removal of a damping element from the momentum equation. This effect is illustrated in Fig. 23: comparing runs 101 and 102 with runs 103 and 104 respectively, it is seen that runs 103 and 104 exhibit a faster reponse to the initiating event. After the initial response, the decreased damping effect is not apparent, probably being masked by the associated alteration of pressure wave behavior, which was the principal purpose behind investigating the variations in nodalization of the dog-leg.

Fig. 24 compares junction 252 mass flow rates for runs using both momentum mixing options and ANGLJ=90 degrees. Dog-leg variation 2A increased the nodalization of the system slightly, and a small difference is seen between variations 2 and 2A in Fig. 25. Dog leg variation 2B increased the nodalization more noticeably, but failed almost immediately. Fig. 26 provides a comparison between dog-leg variation 1, 2, 3, and 4 flow rates at junction 801.

Although the purpose of investigating the variations in dog-leg nodalization was to find a modeling technique which would independently eliminate convergence problems in the downstream region, Table 5 indicates that none was found. Each location of the dog-leg resulted in successful runs in only some of the variations, each momentum mixing option corresponded to a successful run only part of the time, and increasing the system nodalization did not consistently yield a successful run. Because a general solution was not found, two successful dog-leg variations (numbers 2 and 3) are referenced in further discussion of break model 1.

For break model 2, the convergence problems of this section did not arise, and all dog-leg variations tried were successful.

Dog-leg Variation Number	Junction 252 From Volume	Junction 252 Momentum Mixing Option	Other	Success
1	250	Compressible Flow Single Stream	-	N
2	251	Compressible Flow Single Stream	-	Y
2A	251	Compressible Flow Single Stream	Volume 252 Divided Into 2 Equal Vols.	Y
2B	251	Compressible Flow Single Stream	Four Downstream Volumes All Divided Into 2 Equal Volumes	N
2C	251	Compressible Flow Single Stream	Junction 252 ANGLJ=90 deg.	N
3	250	No Momentum Mixing	-	Y
4	251	No Momentum Mixing	-	N

Table 5: Dog-leg Modeling Variations

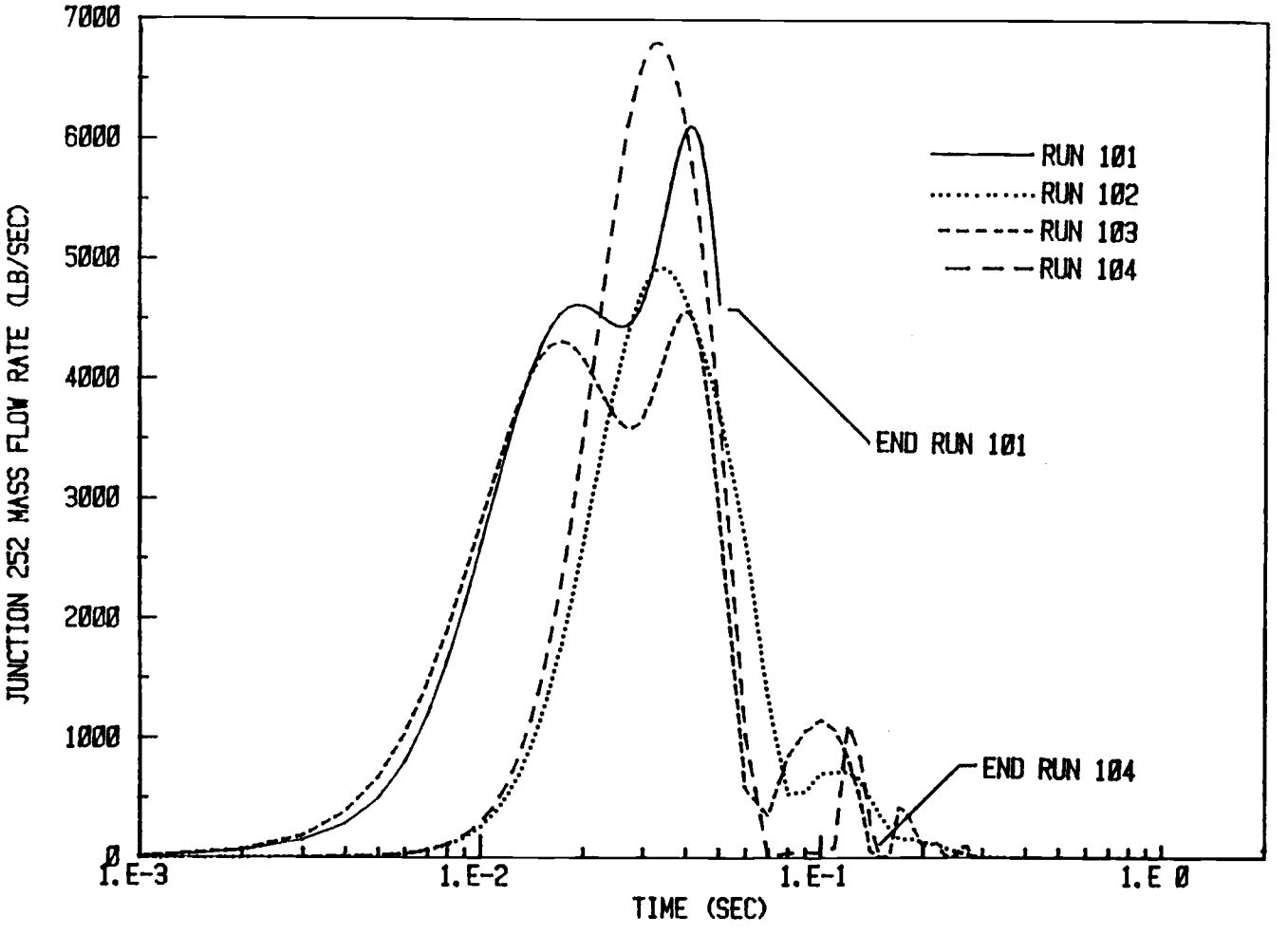

Fig. 23 Junction 252 Mass Flow Rate for a One Millisecond Break

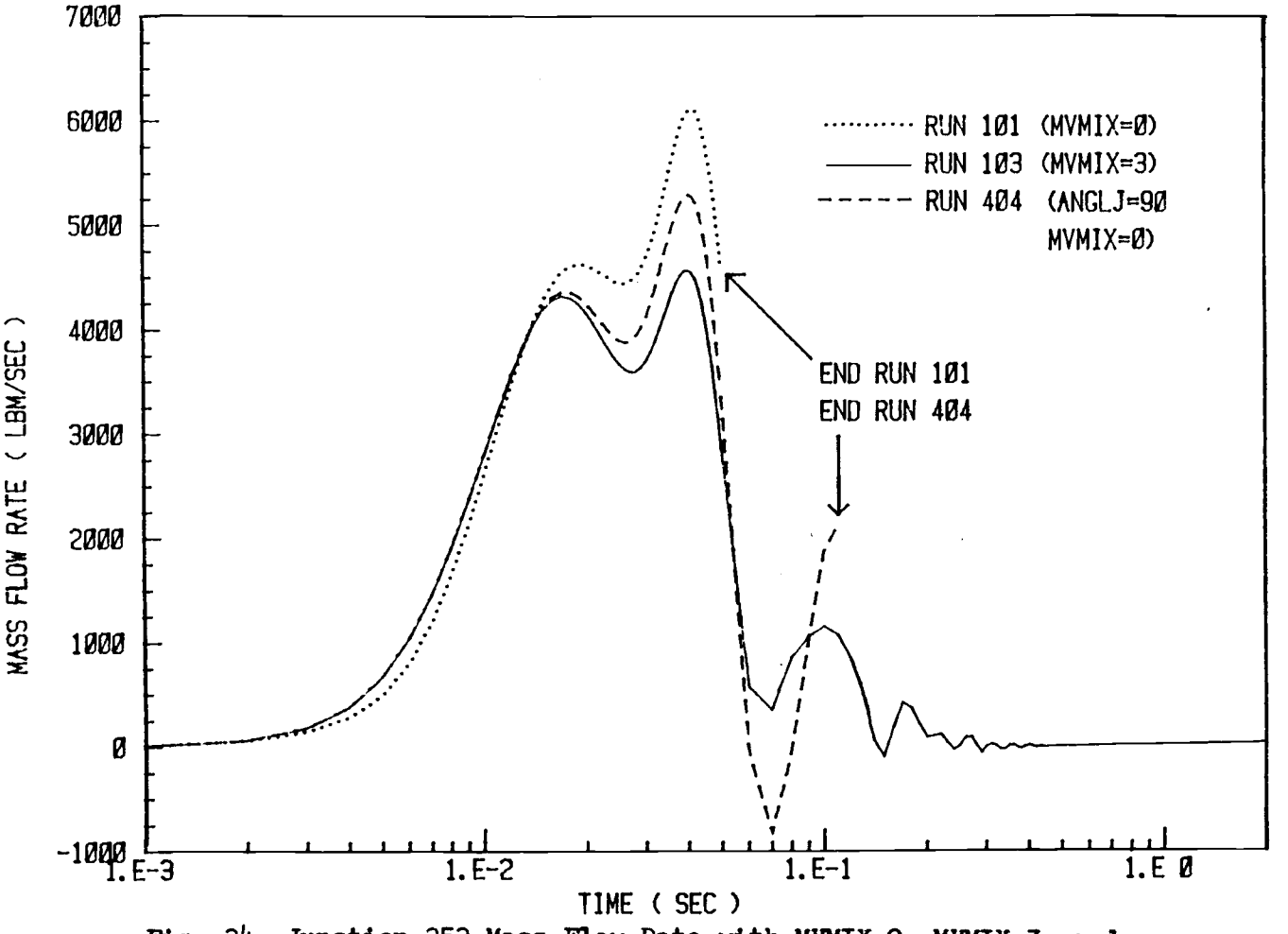

Fig. 24 Junction 252 Mass Flow Rate with MVMIX=0, MVMIX=3, and ANGLJ=90 Degrees (One Millisecond Break)

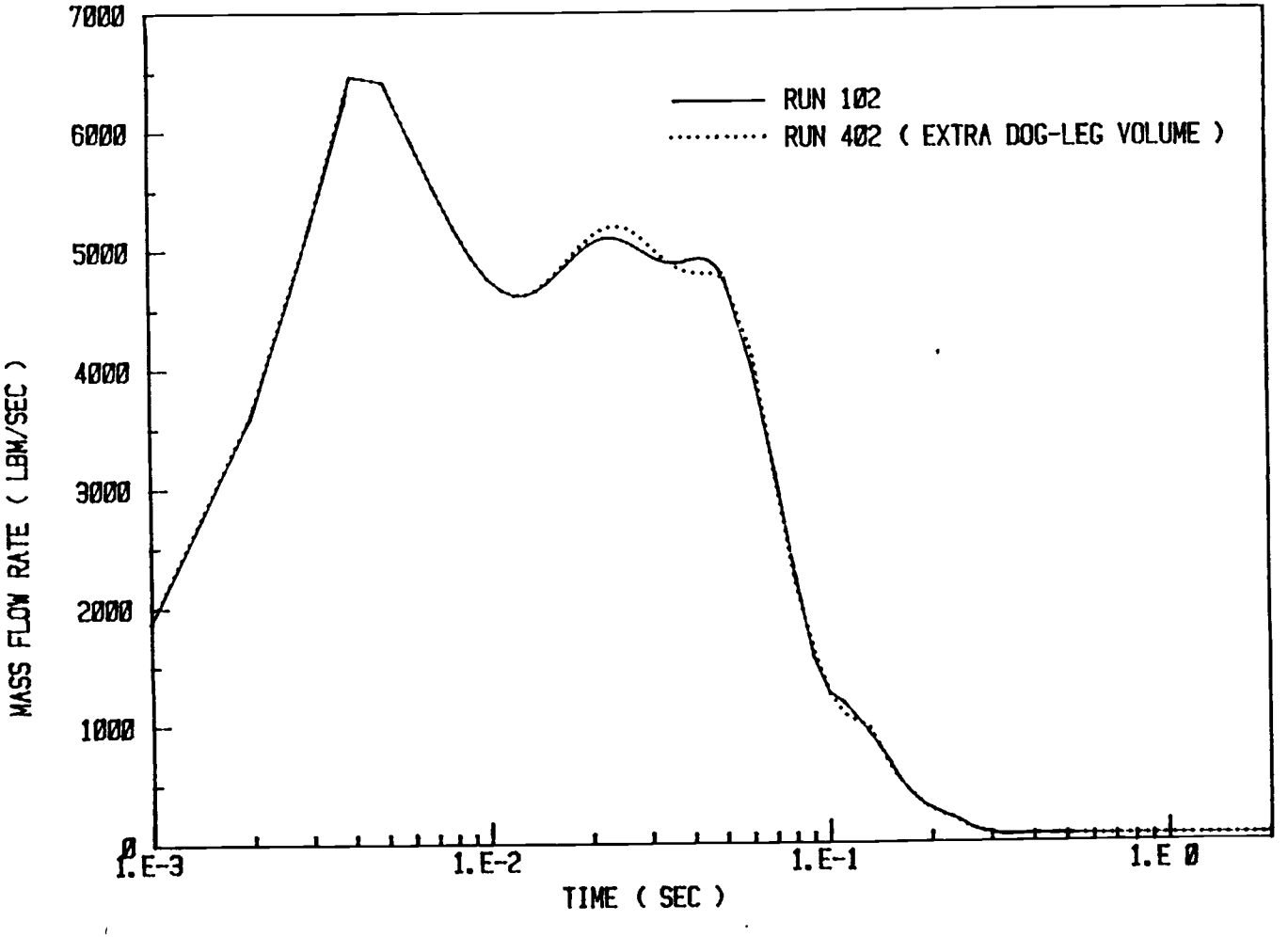

Fig. 25 Junction 801 Mass Flow Rate with and without Extra Volume in Dog-leg

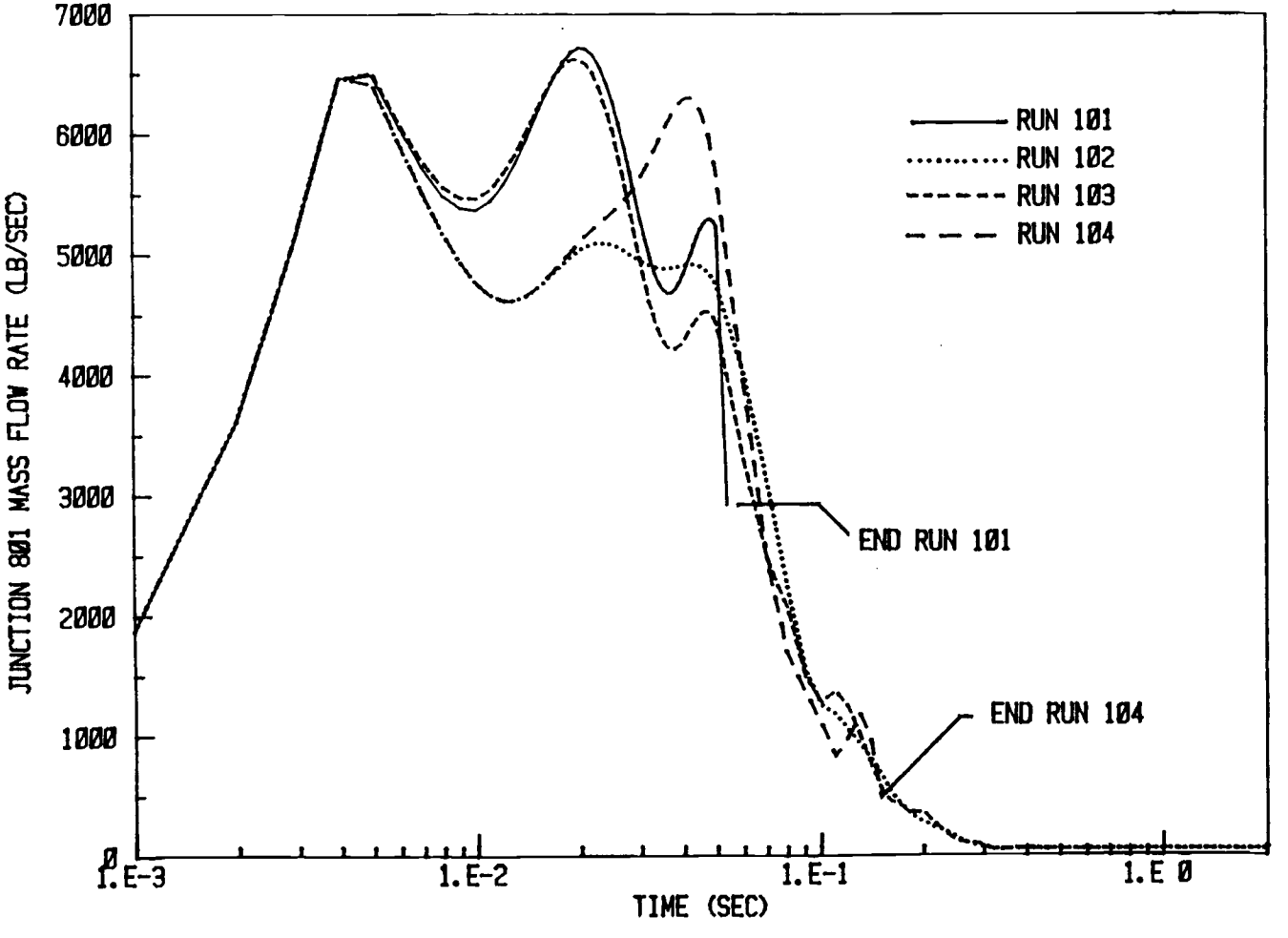

Fig. 26 Junction 801 Mass Flow Rate for a One Millisecond Break

5. Results

Although steam line break model 2 (which includes the penetration volume) is preferred over break model 1 (considering the actual location of the break), the results from both models are presented in this section.

Fig. 27 depicts junction 803 (penetration exit junction) flow for the most conservative break rate (0.001 sec) using dog-leg variations 1, 2, 3, and 4. There is not much variation between the four curves, but run 301 (variation number 1) is the most conservative. It is interesting to note that none of the dog-leg variations failed for this break model: interaction between upstream and downstream sections is provided through volume 803 (the penetration region), where the pressure is relatively high and serves to stop flow through junction 801 (downstream broken end) before evacuation of the downstream section is as complete as occurs with break model 1. Thus, the convergence problems in the downstream section are avoided with break model 2.

Considering the sonic velocity in steam, an appropriate delay for the initial increase of flow in junction 252 is seen in Fig. 23 for runs 102 and 104 considering that junction 252 is located farther from the initiating break for these runs than for runs 101 and 103. Both figures 23 and 26 indicate that for either location of the dog-leg (using break model 1), the case which exhibits more severe oscillations eventually fails. Figures 28 and 29 show junction 801 mass flow rates, quality, and enthalpy for two of the successful dog-leg variations with break model 1. As expected, the quality and enthalpy curves have similar shapes. Depressurization of the downstream section results in generally decreasing enthalpy and quality at junction 801 for the first two tenths of a second; they then climb to their original values after the downstream section has nearly emptied, resulting from the small leak flow persisting at the check valve at junction 251.

As can be seen in Fig. 30, junction 800 flow for break model 1

reaches a maximum at about six milliseconds using a one millisecond break; the flat top on the peak of the flow curve results from linar interpolation between data points by the plotter. Although choking occurs long before the peak, the flow rate continues to rise due to decreasing volume 249 enthalpy. Only one figure for junction 800 conditions is presented since dog-leg variations do not effect results upstream of junction 249 for break model 1 with a one millisecond break ramp (the only break ramp well suited to this model as mentioned previously). Considering the sonic velocity in steam, junction 240 (venturi) flow (Fig. 30) begins a rapid increase at the time the pressure wave initiated by the break arrives. The flow quickly rises to a steady value determined by choked conditions in the flow restrictor at junction 240. Some time after critical flow occurs at junction 240, the effects of the restricted flow are seen downstream where junction 800 flow and volume 249 pressure begin to decrease. Recalling that the Trojan nuclear plant has steamlines of differing lengths, the time delay between break initiation and the limiting of break flow by the flow restrictor implies that breaking the longer steam line (as was done) will give more conservative results (higher mass and energy release rates). Toward the end of the transient, the mass flow rate at junction 240 increases due to decreasing steam quality, and junction 800 flow becomes noticeably less than junctin 240 flow due to lower density fluid at junction 800. Fig. 31 shows junction 800 flow rate, enthalpy, and quality for break model 1.

Because of the critical flow occuring at the break junctions, an interesting comparison can be made between the two steam line break models. Flow conditions at junction 800 (upstream broken end) depend only on upstream fluid conditions once choking occurs, since choking in junction 800 is independent of the presence of volume 803 (penetration volume), except by the indirect path where fluid conditions in volume 803 affect those in volume 250, which in turn affect those in volume 249 (which is upstream from junction 800). However, this indirect path also is not affective when choking in junctions 801 and 249 occurs. Thus, due to the rapidity

of a one millisecond break, the only factor causing noticeably reduced total break flow for break model 2 with respect to break model 1 is the reduced flow at junction 801 resulting from an earlier return from choked conditions at junction 801 due to back pressure in volume 803. Fig. 16 shows that junction 800 mass flow rates for the two break models (runs 201 and 203) are almost identical even for the longer break valve opening rate of Table 4.

Again, figures 13 and 14 show mass flow rate, quality, and enthalpy at junction 803 (break model 2) for a one millisecond break and a break as described in Table 4.

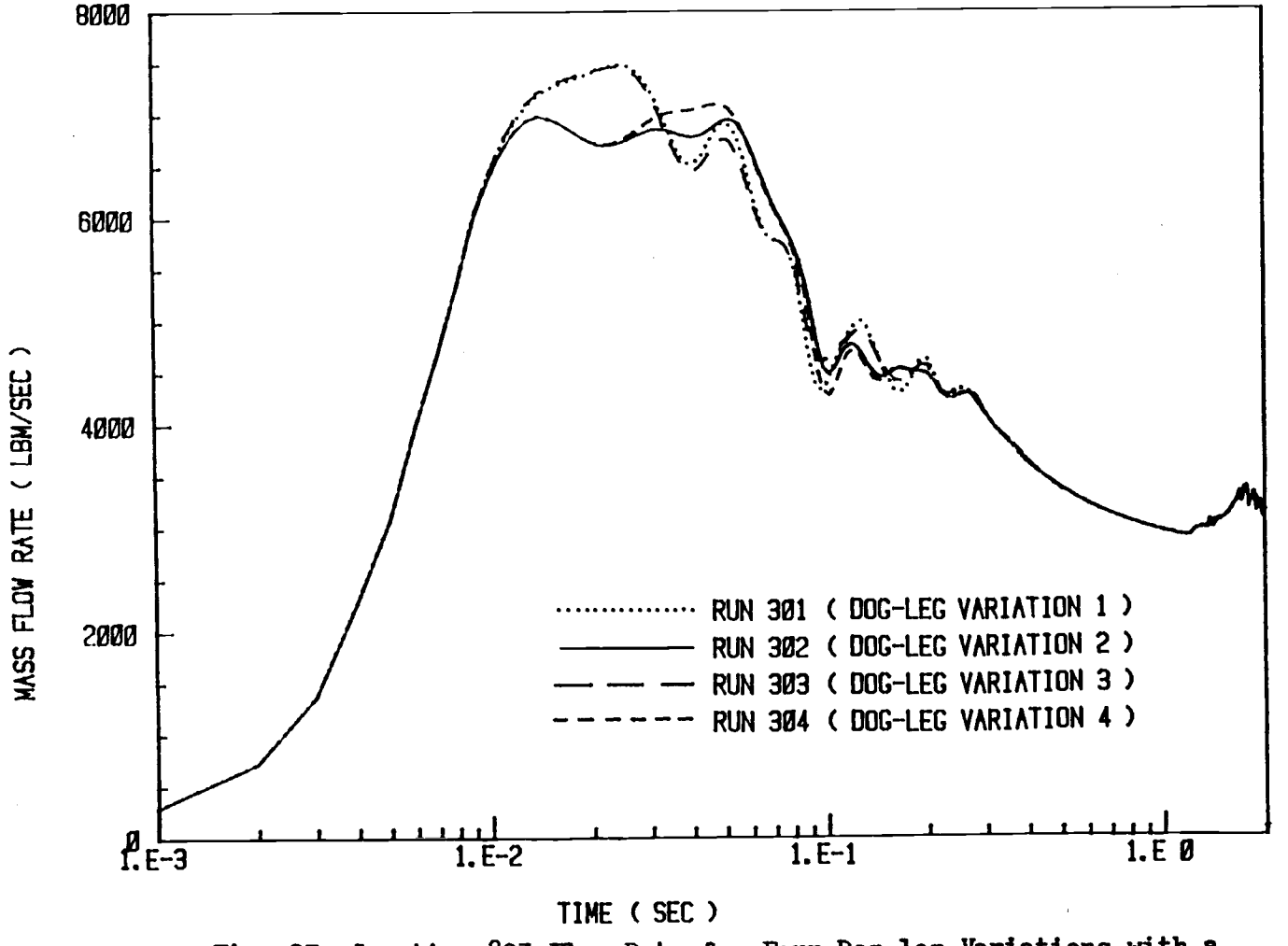

Fig. 27 Junction 803 Flow Rate for Four Dog-leg Variations with a One Millisecond Steam Line Break

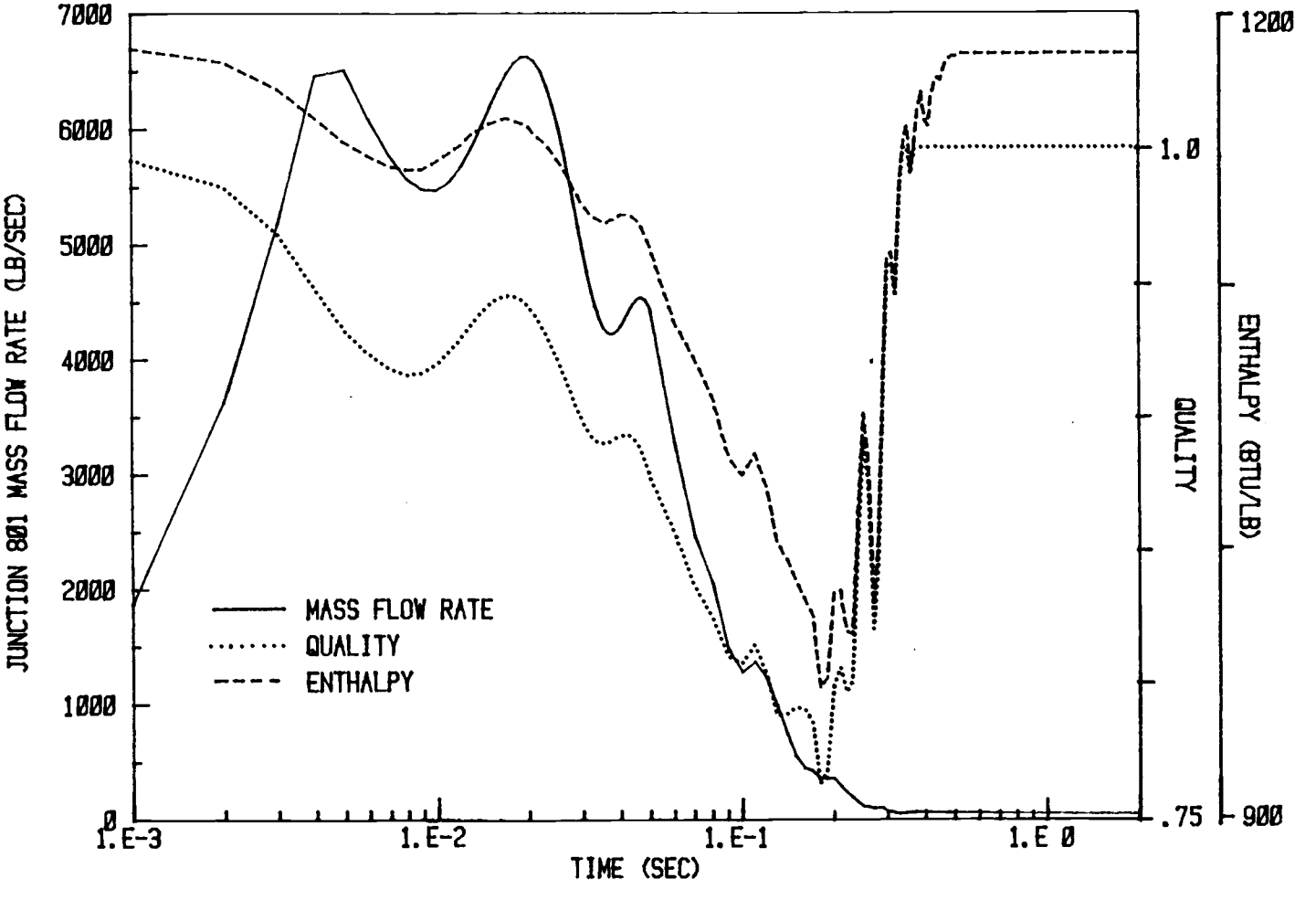

Fig. 28 Junction 801 Mass Flow Rate, Quality, and Enthalpy Vs. Time (Run 103) for a One Millisecond Break

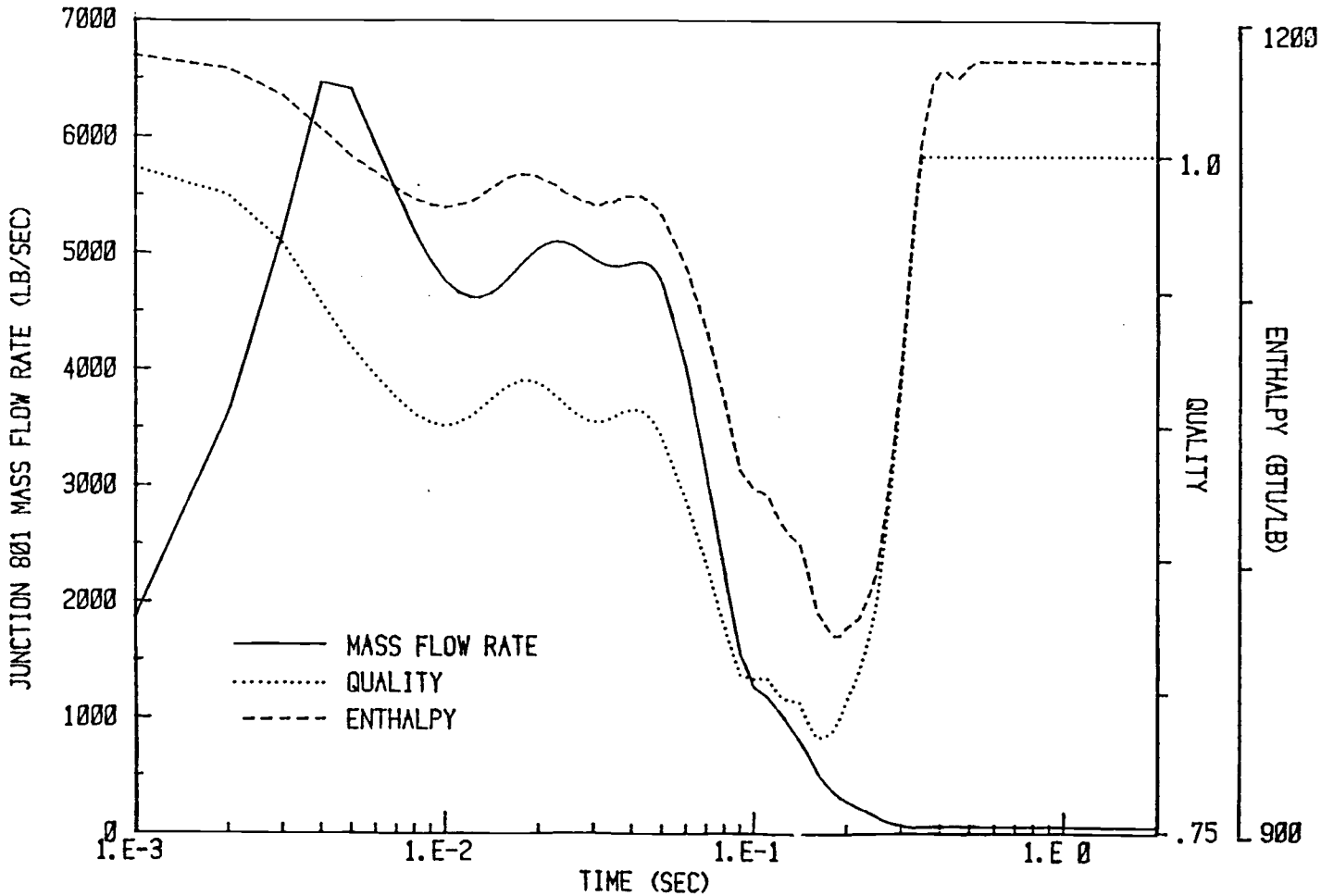

Fig. 29 Junction 801 Mass Flow Rate, Quality, and Enthalpy Vs. Time (Run 102) for a One Millisecond Break

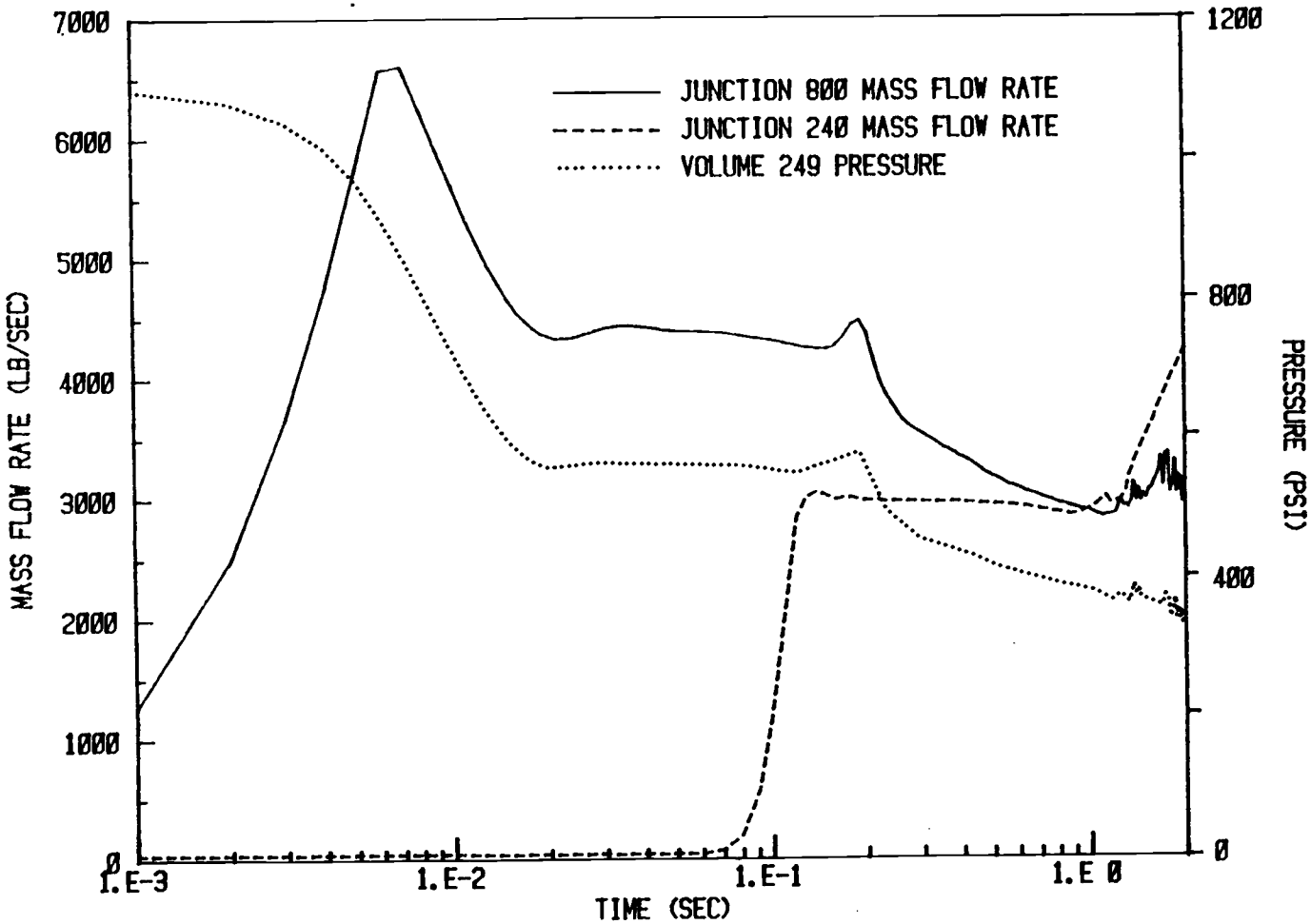

Fig. 30 Junctions 800 and 240 Mass Flow Rates and Volume 249 Pressure for a One Millisecond Break

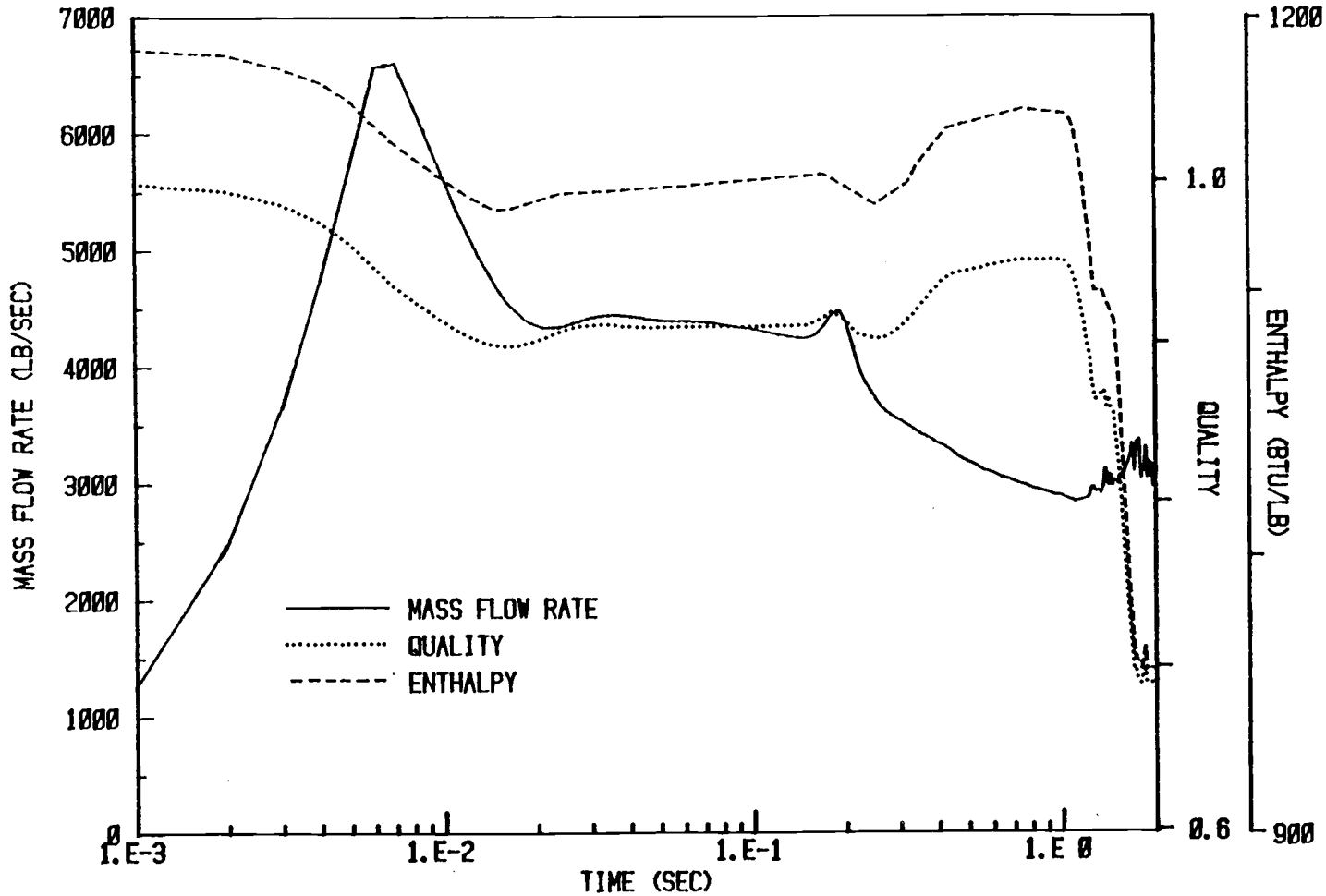

Fig. 31 Junction 800 Mass Flow Rate, Quality, and Enthalpy Vs. Time for a One Millisecond Break

6. Conclusions

An important question which must be raised at this point regards the validity of the various models developed in this study.

One possible actual behavior of the steam line following the break is a diagonal lodging of the downstream section in the penetration region. Break model 2 is obviously well suited to this actual break behavior, with the one millisecond break ramp limiting the severity of the subsequent transient. Any manner in which the broken pipe ends may actually pull away from each other will be less severe than this. However, the break model 2 opening rate sensitivity study (Figures 11 and 12) indicate that selecting a slower break rate will not decrease the conservatism of the results greatly. Should a guillotine break occur outside of the penetration region, break model 1 with a one millisecond break ramp is a conservative representative of actual results.

The second possible behavior is the steam line break followed by ejection of the downstream pipe from the penetration area. As already stated, due to solution uncoupling where choking occurs, ejection of the downstream portion will not affect flow with respect to junction 800 (for break model 2); however, this action will allow the downstream section to vent (completely and rapidly) due to a recuded back pressure, resulting in a flow spike from juncion 801 (downstream broken end). Also, pipe ejection will increase the penetration opening area (junction 803), resulting in a short duration flow increase at junction 803; this flow increase results only from reduction of pressure in volume 803, and as mentioned previously, no effect will be seen at juncion 800. Break model 2 is not appropriate for modeling the pipe ejection phenomenon, and a simple model for representing this action has not been attempted here. In further studies the following model might be tried:

1) a rapid increase of juction 803 area, representing the

increased flow area from the penetration volume following pipe ejection.

2) Close valve 801 and open valve 804 (see below), representing the decrease of flow from the downstream end into the penetration volume accompanied by venting of the downstream region directly to volume 800.

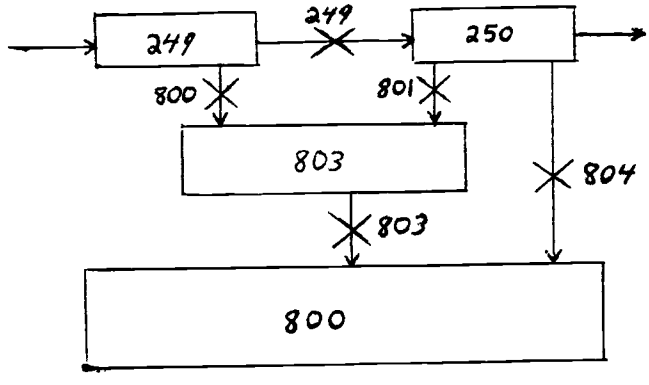

However, this model is not very good since it fails to represent the redirection of flow through a path already open: as flow through valve 801 ceases, flow from valve 804 must accelerate from a value of zero, when in actuality flow from volume 250 would simply increase from the value already present at valve 801 at the time of the ejection. Thus, a much more complicated system would be required to model this phenomenon well.

Comparison of results from this study with the ANS blowdown curve shown in figure 32 indicates that both break models yield results which are substantially lower than those given by the ANS standard. For crude and quick calculations, the ANS curve facilitates a conservative estimate of flow conditions for a guillotine break. However, it is felt that break model 1 gives a more realistic (and still conservative) estimate of actual transient phenomena for a simple guillotine break outide of the penetration region, and that break model 2 gives a realistic (and still conservative) estimate of the blowdown transient when the actual geometry of the break location is considered (excluding the phenomenon of the ejection of the downstream section from the

penetration region).

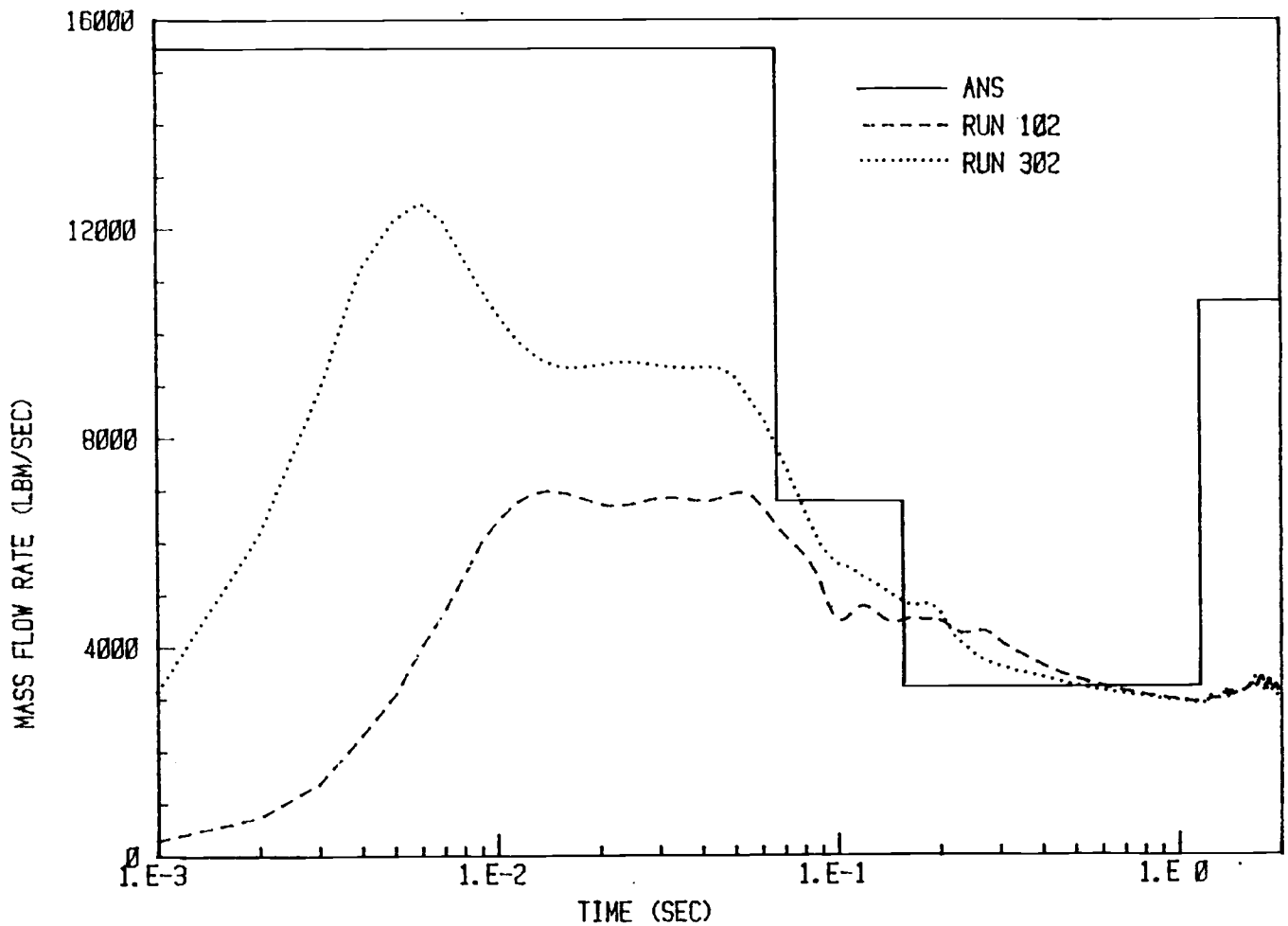

Fig. 32 Comparison of ANS to Break Model 1 and 2 Total Break Flow Rate (One Millisecond Break)

7. References

1. P. B. Chadly. Thermal Hydraulic Analysis of a U-tube Steam Generator in a Pressurized Water Reactor. Oregon State University, May 1983.

2. I. Idel chik. Handbook of Hydraulic Resistance. Israel Program for Scientific Translations Limited, 1966.

3. K. V. Moore et al. RETRAN - A Program for One-Dimensional Transient Thermal-Hydraulic Analysis of Complex Fluid Flow Systems. EPRI NP-408, Vols. 1-4, December 1978.

APPENDICES

8. Appendix I

RETRAN Modeling Corrections

As stated in the forgoing report, the RETRAN model used for this study has been an ongoing development over the past few years. After most of the computer runs used in this paper had been made, a modeling error was discovered which had been passed from reference 1 to the model herein without detection: the enthalpy transport indexes for junctions 23 through 26 and 63 through 66 were all zero. The implications of this error are discussed below:

1) The enthalpy at a junction is calculated by finding the change in enthalpy due to heat transfer and elevation change between the junction and the center of the volume from which the junction flow originates (doner volume). With an enthalpy transport index of zero, heat transfer between doner volume center and junction is ignored, resulting in a slightly lower enthalpy at the junction above each heated secondary volume than at the volume center (due to elevation changes).

2) Because heating is not considered between volume centers and associated exit junctions, heat transferred to each of volumes 23 through 25 and 63 through 65 must be approximately twice the desired amount, since half of the transferred energy is "lost" between volume center and the junction directly above. This implies heat transfer areas larger than necessary.

3) The steady state power output of the system is a known value regardless of enthalpy transport index. Thus, the secondary fluid enthalpy must increase a given amount through the heated volumes, resulting in identical conditions in and above junction 26 during steady state for both correct and incorrect enthalpy transport indexes.

The resulting fluid changes in the heated portion of the steam

generator required the establishment of a new steady state solution for full and then four percent power (a repeat of steps described in the main body of this report). Before establishing the steady state solutions, it was found convenient to make several other alterations to the model: several minor geometry changes were made and published in reference 1 after this study was well under way, and these were incorporated at this point. Another change made was the increase of check valve parameter CV3 from 10**5 to 10**6, reducing the check valve leak flow. Fig. 34 shows the total break flow for a steam line break from the original steady state and a break from the revised steady state described here (with all geometry, check valve, and enthalpy transport index changes). Fig. 33 indicates the effect resulting from correcting the enthalpy transport indexes only (without reestablishing the steady state). The figures show that there is a very minor difference between the cases.

The case chosen in showing the effect of the enthalpy transport indexes was selected due to its relative severity. It is probable that difference would be less for any other case considered in this report.

Because of the small accuracy gain and the considerable amount of computing time and effort required to repeat all runs made previous to this correction, no further effort was made to rectify the situation except to indicate which steady state was used for each run (see appendix II).

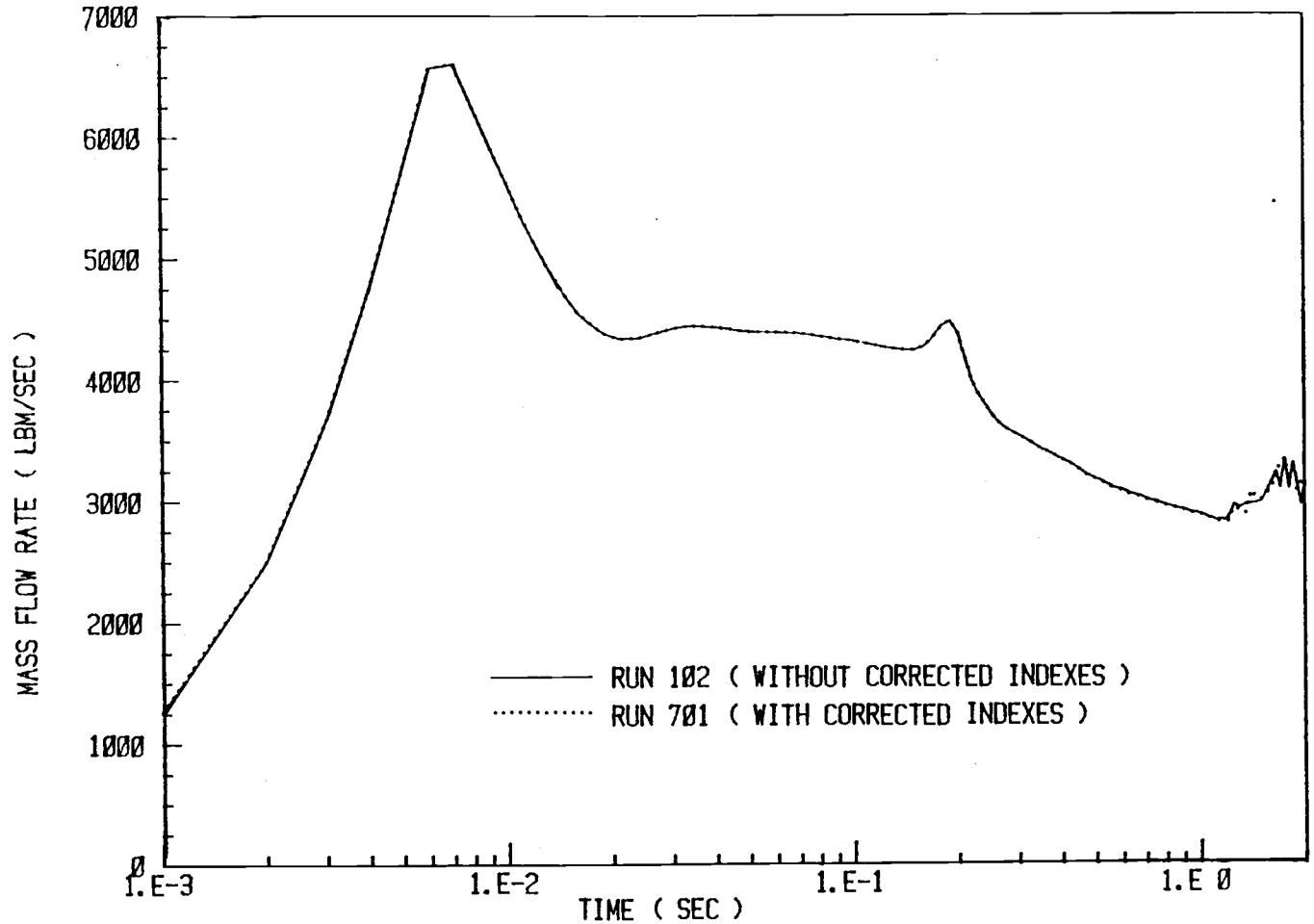

Fig. 33 Junction 800 Mass Flow Rate with and without Correct Enthalpy Transport Indexes (No New Steady State)

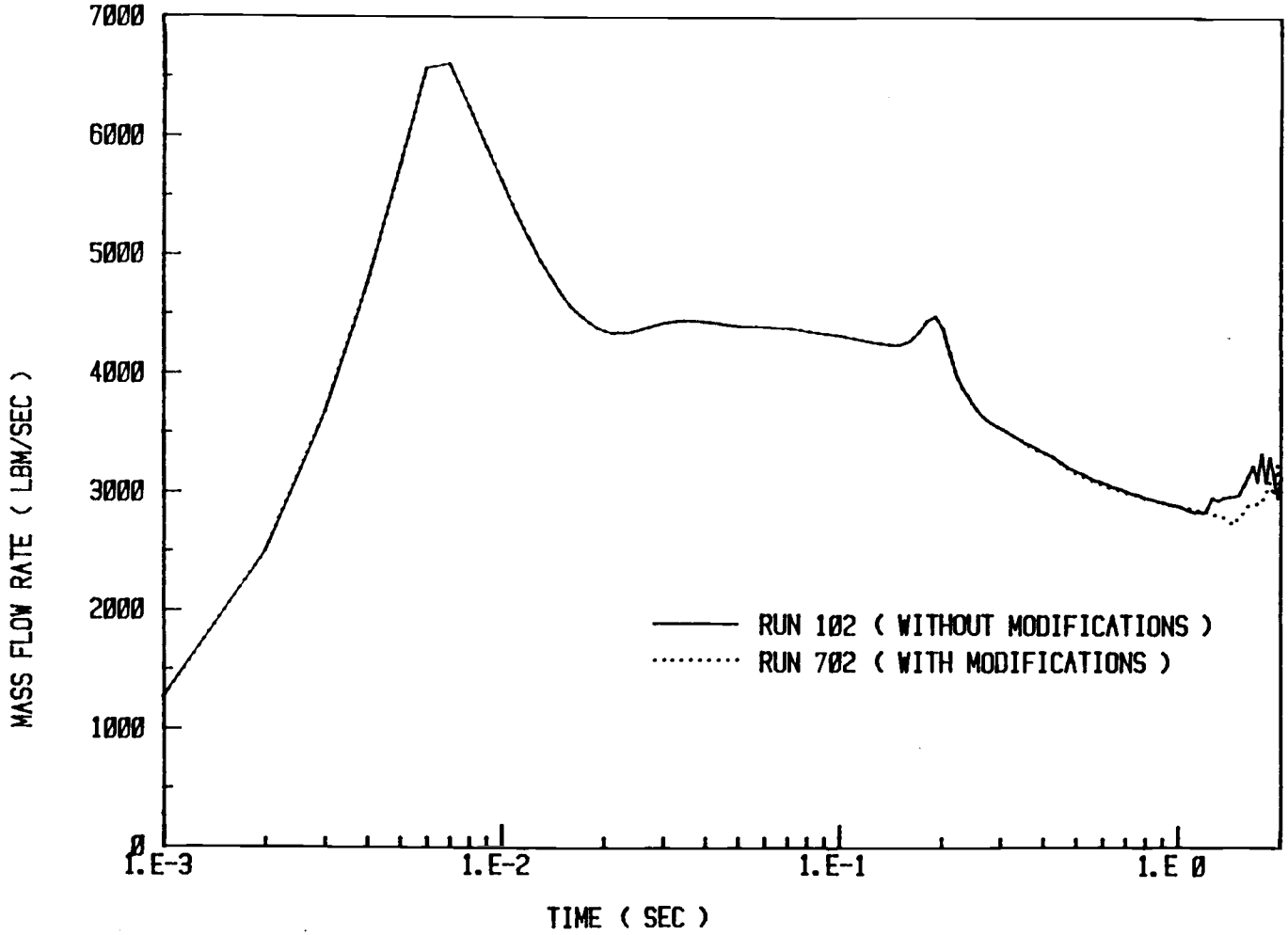

Fig. 34 Junction 800 Mass Flow Rate with and without Correct Enthalpy Transport Indexes and Geometry Changes

9. Appendix II

Characteristics of RETRAN Runs

Table 6 describes the distinguishing charcteristics of all RETRAN runs for which figures are presented in this report. A "Y" in the success column indicates that the run completed the entire two second transient. A "Y" in the "Appendix I Enthalpy Transport" column indicates that the correct enthalpy transport indices and the corresponding steady state were used. The break options and dog-leg (relief valve header) options are described in the main body of this report.

Run No.	Break Model No./Dog-leg Variation No.	Break Opening Rate	Appendix I Enthalpy Transport/ Success	Other
101	1 / 1	0.001 sec	N / N	-
102	1 / 2	0.001 sec	N / Y	-
103	1 / 3	0.001 sec	N / Y	-
104	1 / 4	0.001 sec	N / N	-
201	1 / 2	Table 4	N / Y	-
202	2 / 2	Table 4	Y / Y	No Choke Jun. 800 & 801
203	2 / 2	Table 4	N / Y	-
204	2 / 2	Table 4	Y / N	No Choke Jun. 249
301	2 / 1	0.001 sec	N / Y	-
302	2 / 2	0.001 sec	N / Y	-
303	2 / 2	0.001 sec	N / Y	-
304	2 / 4	0.001 sec	N / Y	-
401	1 / 2	0.001 sec	N / Y	Vol. 252 Divided in Two
402	1 / 3	0.001 sec	N / N	4 Downstream Vols. Divided in Two
403	1 / 3	0.001 sec	N / Y	Jun. 800 & 801 Ixl.5
403A	1 / 2	Table 4	N / Y	Jun. 800 & 801 Ixl.5
404	1 / 1	0.001 sec	N / N	Jun. 252 ANGLJ=90 deg.
405	1 / 3	0.001 sec	N / N	Jun. 800 & 801 Moody Choking
406	1 / 3	0.001 sec	N / N	No Choke Jun. 800 & 801
407	1 / 2	0.001 sec	Y / Y	Jun. 800 & 801 Loss Coefficient x 0.25
408	1 / 2	0.001 sec	Y / Y	Jun. 800 & 801 Loss Coefficient x 4.0
501	1 / 2	Table 4 tx0.75	N / Y	-
502	1 / 2	Table 4 txl.25	N / Y	-
503	1 / 2	Table 4 tx0.50	N / Y	-
601	2 / 2	Table 4 tx0.75	N / Y	-
602	2 / 2	Table 4 txl.25	N / Y	-
603	2 / 2	Table 4 tx0.50	N / Y	-
701	1 / 2	0.001 sec	N / Y	Enthalpy Transport Indexes Added to Original Steady State
702	1 / 2	0.001 sec	Y / Y	-

Table 6. Description of Runs Incorporated in Plots